MODEL STUDIES OF TIDAL EFFECTS ON GROUND WATER HYDRAULICS

by

John A. Williams

Ronald N. Wada

Ru-yih Wang

Technical Report No. 39

May 1970

Project Completion Report

of

TIDAL EFFECTS ON GROUND-WATER HYDRAULICS IN HAWAII

OWRR Project No. A-015-HI, Grant Agreement No. 14-01-0001-1630

Principal Investigators: John A. Williams, L. Stephen Lau and Doak C. Cox

Project Period: February 1968 to June 1969

The programs and activities described herein were supported in part by funds provided by the United States Department of the Interior as authorized under the Water Resources Act of 1964, Public Law 88-379.

ABSTRACT

This report presents the results of a model study on the propagation of periodic fluctuations in the piezometric head through a saturated porous media. Three different models were employed: a hydraulic model, a mathematical model, and an electrical analog model. The hydraulic model consisted of one or more layers of polyurethene foam placed in a lucite tank. The foam was tested in a confined and unconfined condition using both a no-flow and a constant-head boundary condition at the internal boundary. The mathematical and electric analog models duplicated the conditions in the hydraulic model.

The results of the study indicate that diffusion theory can describe the propagation of such disturbances provided that the boundary conditions are satisfied and that the correct diffusion coefficient is employed. The calculation of the correct diffusion coefficient requires that an appropriate storage coefficient and an apparent porosity be used for the confined and unconfined models, respectively.

For the unconfined case, the ratio of the apparent porosity to the true porosity is of the same order of magnitude for both the polyurethene foam and a Sacramento River sand.

CONTENTS

LIST OF FIGURES

LIST OF TABLES

INTRODUCTION

In the development of ground-water aquifers, the coefficients of storage and transmissability in the large are required. These coefficients are usually determined from pumping-test data which yield reasonably accurate values of the transmissability coefficient but which produce values for the storage coefficient which may be considerably in error. In aquifers in coastal regions which are in communication with the sea, tidal changes produce fluctuations in the piezometric head which, if measured, could be used to determine the ratio of storage to transmissability. If pumping-test data were available to give the transmissability, the storage could then be estimated.

Thus, the objective of this research was to investigate a technique for determining the ratio of storage to transmissability which employs the response of coastal aquifers to tidal changes. To accomplish this, both hydraulic and electric analog models of aquifers of simple boundary geometry were used and measurements of the amplitude and phase of tidal-generated fluctuations in the piezometric surface were compared with the amplitude and phase as predicted from the corresponding mathematical models.

Related previous work has been done by Werner and Noren (1951). They have derived the mathematical model for an unconfined one-dimensional aquifer, based on Dupuit's assumption of a constant hydraulic gradient in any vertical section. They compared the ratio of the decay factors for semi-diurnal and nine-day tidal periods with records by E. Prinz (1923) of water-surface fluctuations in wells adjacent to the Elbe River. The mathematical model predicted that the semi-diurnal tide should decay about four times as fast with respect to distance from the river as the nine-day tide. Measurements from the records indicated that this ratio is around 2.0.

Todd (1954) has carried out an experimental investigation of unsteady flow in unconfined aquifers using a 10-foot by 1.5-foot vertical Hele-Shaw model. More specifically, he investigated the propagation of transient disturbances produced by a sudden increase, a sudden decrease, and a solitary sine-wave fluctuation of the piezometric surface in the forebay of the model. For the tests with the solitary sine wave, a constant oil depth of 6.6 to 6.9 cm was maintained at the outflow boundary. The heights of the waves varied from 2.5 to 15.2 cm and their periods, from 2 to 6 minutes.

Miller (1941) conducted experiments in a hydraulic model where the porous media was Sacramento River (California) sand having a grain-size diameter which varied from 0.074 mm to 1.20 mm with a median diameter of about 0.44 mm and a porosity of 0.345. The section of the model containing the media was 9.6 feet long by 1.0 foot wide by 1.5 feet deep. A solid wall provided a no-flow boundary condition at the interior end of the test section. Fluctuations in the forebay were sinusoidal in time with periods of either five or ten minutes. Miller's general experimental set-up was essentially the same as the hydraulic model tests utilized in the study reported here. The only difference is the porous media used.

THE MATHEMATICAL MODEL

The Basic Differential Equations

The application of the conservation of mass principle and Darcy's Law to an isotropic and homogeneous porous media, saturated between the surfaces z = 0 and z = z (x, y)[1], yields two basic differential equations:

$$\nabla \cdot (z\nabla h) = \frac{z}{K} w_o \left(\frac{1}{E} + \frac{\varepsilon}{\beta}\right) \frac{\partial h}{\partial t} = \frac{S_s}{K} \frac{\partial h}{\partial t} \quad , \tag{1a}$$

and

$$\nabla \cdot (z\nabla z) = \frac{\varepsilon'}{K} \frac{\partial z}{\partial t} \quad . \tag{1b}$$

Equation (1a) applies to confined aquifers where h is a function of (x,y) and represents the piezometric surface. The quantities E, ε, and K are Young's modulus of the media, the porosity of the media, and the Darcy coefficient of permeability, respectively. β and w_o are the bulk modulus and the specific weight of water, respectively. The quantity $w_o(1/E + \varepsilon/\beta)$ is defined as the specific storage, S_s, and represents the volume of water that a unit decline in head releases from storage from a unit volume of media. This equation was first derived by C. E. Jacob (Jacob, 1950, Chapter 5).

---

[1] All symbols used are summarized in Appendix A.

Equation (1b) applies to unconfined aquifers where compressibility of the water is considered negligible and where the upper surface of the water and the piezometric surface coincide, hence, $z \equiv h$. If the capillary fringe zone is neglected $z = z(x,y)$ defines the phreatic surface and ε becomes ε', the apparent porosity. K is again the Darcy permeability of the media. This equation is known as Boussinesq's equation of unsteady flow and the details of its derivation may be found in Chapter 8 of *Physical Principles of Water Percolation and Seepage* (Bear, *et al.*, 1968, Chapter 8).

Both equations (1a) and (1b) are based on the assumption that the streamline curvature of the flows involved will be small enough to prevent any density gradients.

The Phreatic, One-dimensional, Finite Aquifer

If there is no variation of the flow in the y-direction, if the changes in the elevation of the phreatic surface with respect to the average depth are very small (i.e., $\zeta = z - \bar{z} \ll 1$), and if the slope of the phreatic surface always remains small (i.e., $\partial z/\partial x \ll 1$), then equation (1b) can be written

$$\frac{\partial^2 \zeta}{\partial x^2} = \frac{\varepsilon'}{K\bar{z}} \frac{\partial \zeta}{\partial x} \quad . \tag{2a}$$

If there is a periodic dependence on time, then $\zeta(x,t) = R[\eta(x)e^{i\sigma t}]$ and equation (2a) reduces to

$$\frac{d^2\eta}{d x^2} - i\alpha\eta = 0, \ \alpha = \frac{\varepsilon'\sigma}{K\bar{z}} \quad . \tag{2b}$$

This equation has solutions in the form,

$$\eta = C_1 e^{\sqrt{i\alpha}\, x} + C_2 e^{-\sqrt{i\alpha}\, x} \quad , \tag{2c}$$

where C_1 and C_2 are complex constants to be determined from the boundary conditions.

For the boundary condition, $\zeta(L,t) = \zeta(-L,t)$, $C_1 = C_2$ (this is the same as requiring $\partial\zeta/\partial x = 0$ or no-flow at $x = 0$), and

$$\zeta(x,t) = R[e^{i\sigma t} C_3 \cosh\sqrt{i\alpha}\, x] \quad . \tag{3a}$$

Finally, if the boundary condition at $x = L$ is $\zeta(L,t) = R(-i\zeta_o e^{i\sigma t})$ then $C_3 = -i\zeta_o/\cosh\sqrt{i\alpha}\,L$ and the solution becomes

$$\zeta(x,t) = R[-e^{i\sigma t}\, i\zeta_o \cosh\sqrt{i\alpha}\,x/\cosh\sqrt{i\alpha}\,L] \tag{3b}$$

or

$$\zeta(x,t) = \frac{\zeta_o}{4}\,\frac{A + B + C + D}{\sinh^2\sqrt{\frac{\alpha}{2}} + \cos^2\sqrt{\frac{\alpha}{2}}\,L} \tag{3c}$$

where

$$A = e^{\sqrt{\frac{\alpha}{2}}(x + L)}\sin[\sqrt{\tfrac{\alpha}{2}}\,(x - L) + \sigma t]$$

$$B = e^{\sqrt{\frac{\alpha}{2}}(x - L)}\sin[\sqrt{\tfrac{\alpha}{2}}\,(x + L) + \sigma t]$$

$$C = e^{-\sqrt{\frac{\alpha}{2}}(x - L)}\sin[-\left(\sqrt{\tfrac{\alpha}{2}}\,(x + L) - \sigma t\right)]$$

$$D = e^{-\sqrt{\frac{\alpha}{2}}(x + L)}\sin[-\left(\sqrt{\tfrac{\alpha}{2}}\,(x - L) - \sigma t\right)] \quad .$$

This is the form of the solution found by Werner and Noren (1951) where A and B are right-traveling disturbances and C and D are left-traveling disturbances. This solution can be put into a second form which is more convenient for numerical calculations, i.e.,

$$\zeta(x,\, t) = \zeta_o\rho\sin(\sigma t + \Theta_p) \quad , \tag{4a}$$

where

$$\rho = \sqrt{\frac{\cos^2\sqrt{\frac{\alpha}{2}}\,x + \sinh^2\sqrt{\frac{\alpha}{2}}\,x}{\cos^2\sqrt{\frac{\alpha}{2}}\,L + \sinh^2\sqrt{\frac{\alpha}{2}}\,L}}$$

and

$$\tan\Theta_p = \frac{\tanh\sqrt{\frac{\alpha}{2}}\,x\,\tan\sqrt{\frac{\alpha}{2}}\,x - \tanh\sqrt{\frac{\alpha}{2}}\,L\,\tan\sqrt{\frac{\alpha}{2}}\,L}{1 + \tan\sqrt{\frac{\alpha}{2}}\,x\,\tanh\sqrt{\frac{\alpha}{2}}\,x\,\tan\sqrt{\frac{\alpha}{2}}\,L\,\tanh\sqrt{\frac{\alpha}{2}}\,L} \tag{4c}$$

If the boundary condition at $x = 0$ were that of a constant head, then $C_1 = -C_2$ in equation (2c) and the following equations for ρ and Θ_p result:

$$\rho = \sqrt{\frac{\sin^2\sqrt{\frac{\alpha}{2}}\,x + \sinh^2\sqrt{\frac{\alpha}{2}}\,x}{\sin^2\sqrt{\frac{\alpha}{2}}\,L + \sinh^2\sqrt{\frac{\alpha}{2}}\,L}} \tag{5a}$$

and

$$\tan \Theta_p = \frac{\coth \frac{\alpha}{2} x \tan \frac{\alpha}{2} x - \coth \frac{\alpha}{2} L \tan \frac{\alpha}{2} L}{1 + \coth \frac{\alpha}{2} x \tan \frac{\alpha}{2} x \coth \frac{\alpha}{2} L \tan \frac{\alpha}{2} L} \qquad (5b).$$

The Phreatic, One-Dimensional, Cylindrical Island Aquifer

If there is no variation of the flow in the tangential direction, if the changes in the phreatic surface are small with respect to some average depth, and if the slope of the phreatic surface again remains small, then equation (1b) can be written

$$\frac{1}{r}\frac{\partial}{\partial r}\left(r\frac{\partial \zeta}{\partial r}\right) = \frac{\varepsilon'}{K\bar{z}}\frac{\partial \zeta}{\partial t} \quad ; \; \zeta = z - \bar{z} \; . \qquad (6a)$$

If a periodic time variation is assumed as previously, then (6a) reduces to

$$\frac{d}{dr}\left(r\frac{d\eta}{dr}\right) - i\alpha r\eta = 0 \; ; \; \alpha = \frac{\varepsilon'\sigma}{K\bar{z}} \; . \qquad (6b)$$

This is a modified Bessel's Equation and has solutions of the form,

$$\eta(r) = C_1 J_0(i^{3/2}\sqrt{\alpha}\, r) + C_2 Y_0(i^{3/2}\sqrt{\alpha}\, r) \quad , \qquad (6c)$$

where C_1 and C_2 are complex constants determined by boundary conditions. At $r = 0$, $\zeta(r,t)$ should remain bounded, hence, C_2 must be zero. If the radius of the island, L, is small with respect to the tidal wave length, no appreciable phase difference in the water-surface elevation will be observed around the island and the boundary condition at $r = L$ can be expressed as $\zeta(L,t) = R(-i\zeta_o e^{-i\sigma t})$. If these boundary conditions are applied to equation (6c) together with the identity, $J_0(i^{3/2}x) = \text{ber}x + i\text{bei}x$, and the result multiplied by $e^{i\sigma t}$, then the real part of the product is $\zeta(r,t)$, that is,

$$\zeta(r,t) = \zeta_o \rho \sin(\sigma t - \Theta_p) \; , \qquad (7a)$$

where

$$\rho = \sqrt{\frac{\text{ber}^2 \sqrt{\alpha}\, r + \text{bei}^2 \sqrt{\alpha}\, r}{\text{ber}^2 \sqrt{\alpha}\, L + \text{bei}^2 \sqrt{\alpha}\, L}} \; , \qquad (7b)$$

and

$$\tan\Theta_p = \frac{\text{ber}\sqrt{\alpha}\, L \,\text{bei}\sqrt{\alpha}\, r - \text{bei}\sqrt{\alpha}\, L\, \text{ber}\sqrt{\alpha}\, r}{\text{ber}\sqrt{\alpha}\, r\, \text{ber}\sqrt{\alpha}\, L + \text{bei}\sqrt{\alpha}\, r\, \text{bei}\sqrt{\alpha}\, L} \qquad (7c)$$

The Confined, One-Dimensional, Finite Aquifer

If the aquifer is of constant thickness, i.e., $z(x,y) \equiv b$, and if there is no variation of the flow in the y direction, equation (1a) becomes

$$\frac{\partial^2 h}{\partial x^2} = \frac{S_s}{K}\frac{\partial h}{\partial t} = \frac{S}{T}\frac{\partial h}{\partial t} \quad . \tag{8a}$$

For periodic time dependence, then $h(x,t) = R[\eta(x)e^{i\sigma t}]$, and equation (8a) reduces to

$$\frac{d^2\eta}{d\,x^2} - i\alpha\eta = 0 \;;\; \alpha = \frac{\sigma S}{T} \quad . \tag{8b}$$

This is exactly the same as equation (2b), hence, the solutions previously determined for equation (2b) apply here, provided the proper expression for α is used. Specifically, equation (3c) or its counterparts, equations (4a), (4b), and (4c), represent the one-dimensional confined aquifer with a no-flow boundary condition at $x = 0$, and equations (5a) and (5b) apply to the confined aquifer with a constant-head boundary condition at $x = 0$.

The Confined, One-Dimensional Cylindrical Island Aquifer

If the aquifer is of constant thickness, if there is no variation of the flow in the tangential direction, and if changes in time are periodic, then equation (1a) becomes

$$\frac{d}{dr}\left(r\frac{d\eta}{dr}\right) - i\alpha r\eta = 0 \;;\; \alpha = \frac{S\sigma}{T} \quad . \tag{9}$$

Thus, the solutions for the phreatic island-aquifer, i.e., equations (7a), (7b), and (7c) are valid when used with the correct expression for α.

It should be noted that the solutions for the one-dimensional aquifers with the no-flow boundary condition are also solutions for aquifers of length 2L, having the same periodic variation in piezometric surface applied at both ends, $x = \pm L$. The solutions for the several aquifers and their boundary conditions are summarized in Figure 1.

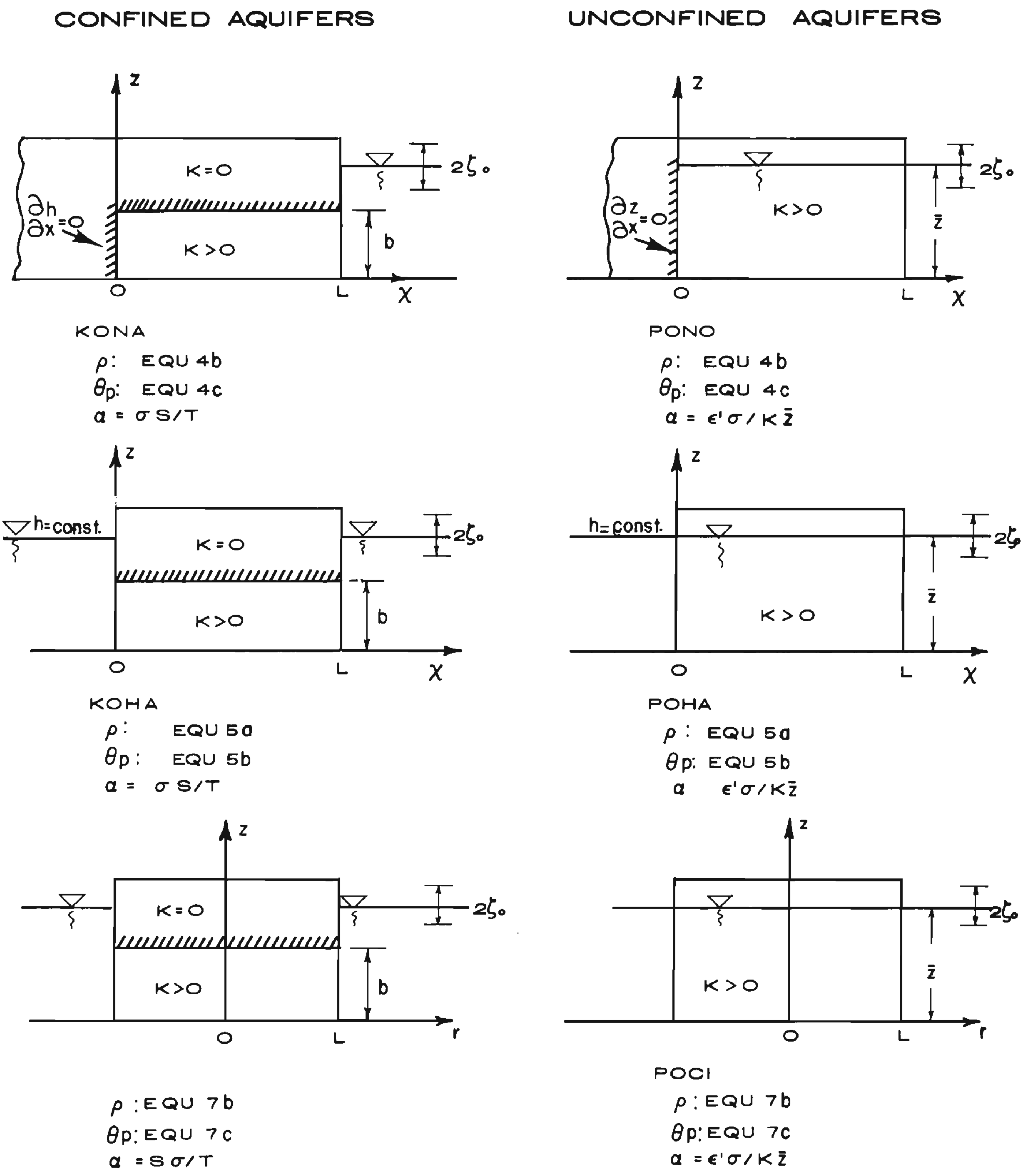

FIGURE 1. SUMMARY OF MATHEMATICAL MODELS.

The Electric Circuit Analog

For a confined aquifer of constant thickness and an unconfined aquifer whose depth differs only slightly from some average value, $\bar{z}$, the equations (1a) and (1b) take the form,

$$\frac{\partial^2 h}{\partial \bar{x}^2} = a^2 C_D \frac{\partial h}{\partial t} \quad , \tag{10}$$

where $C_D = S/T$ for the confined aquifer, $C_D = \varepsilon'/K\bar{z}$ for the unconfined aquifer, and $x = \bar{x}/a$ is a new variable which measures in "a" feet units of length.

The following conversion factors relate the corresponding hydraulic and electrical quantities:

$$q\ (ft^3) = K_1 \mathcal{Q}\ (\text{coulombs}), \tag{11a}$$
$$h\ (ft) = K_2\ V\ (\text{volts}), \tag{11b}$$
$$Q\ (cfs) = K_3 i\ (\text{amps}), \tag{11c}$$
$$t\ (sec) = K_4 t_e\ (sec), \tag{11d}$$

where $q = Q\ t$ requires

$$K_1 = K_3 K_4 . \tag{12}$$

Making use of equations (11b) and (11d) and considering a one-dimensional flow, equation (10) transforms into

$$\frac{\partial^2 V}{\partial \bar{x}^2} = \frac{a^2 C_D}{K_4} \frac{\partial V}{\partial t_e} = a^2 C_D \frac{K_3}{K_1} \frac{\partial V}{\partial t_e} \quad . \tag{13}$$

The flow of electricity in a circuit composed of a parallel plate capacitor with one plate acting as conductor requires that

$$a^2 C_D \frac{K_3}{K_1} = RC \quad , \tag{14}$$

where R and C are the resistance and capacitance per unit length of the capacitor plate, respectively.

To relate C_D with R and C the analogy between Ohm's Law and Darcy's Law is used, i.e.,

$$Q/\text{ft. width} = T \frac{\Delta h}{\Delta \bar{x}} \text{ and } i = \frac{1}{R} \frac{\Delta V}{\Delta \bar{x}} \quad ,$$

where $\Delta\bar{x}$ is the distance over which the head drop Δh takes place in the hydraulic system and the distance over which the voltage drop ΔV takes place in the electrical system. Application of equation (11) to these two laws yields the relation,

$$RT = K_3/K_2 \quad . \tag{15}$$

Eliminating RT between equation (15) and (14) and taking C_D for a confined aquifer results in

$$C = \frac{K_2}{K_1} a^2 S \quad . \tag{16}$$

Equations (14), (15), and (16) provide the necessary relations for the determination of the electric analog for a given aquifer. That is, K_2 is fixed and then K_3 is selected in equation (15) to give a convenient value for R. K_1 is likewise selected to give a convenient value of C, using equation (16). Finally, for the determined values of R and C, the time scale factor K_4 is found from equation (12). The distance "a" represents the grid spacing in the finite difference approach to the solution of equation (10). For the unconfined aquifer, the same equations that are valid if S is replaced by ε' and T is replaced by $K\bar{z}$.

EXPERIMENTAL APPARATUS AND PROCEDURE

The Hydraulic Model

The hydraulic model consisted of a lucite tank 6.0 inches wide by 64.0 inches long by 18.0 inches deep. At each end a compartment 8.0 inches in length could be formed by inserting removable bulkheads. A cylindrical plunger, made from five-inch diameter PVC pipe, was located at one end of the tank. This plunger was driven by a 1/4 hp, B & B variable-speed motor (254 inch-pound torque) and an S-47 model electronic controller which activated a driving rod connected to a yoke and flywheel assembly. The motor speed could be varied from about 4 to 40 rpm, and the amplitude on the plunger displacement could be varied from 0 to 4 inches. Two inches from the bottom of the tank and along one side of it, a series of pressure taps was drilled. The first twelve taps were spaced two inches apart from center to center, with the exception of Taps 4 and 5 which were 2.25 inches apart. The last four taps were spaced six inches from center to center. Each tap was connected through a needle valve and a piece of copper tubing to a one-inch PVC pipe manifold. A single tap was drilled in the end compartment containing the tidal plunger. The manifold and the tidal compartment were each connected with a piece of Imperial 44-P-1/4 tubing to Statham Gold-cell transducers. Each Gold-cell was used with a 0-2.0 psi range pressure diaphragm. The pressure transducers, in turn, were connected to a two-channel Hewlett-Packard model no. 321 recording oscillograph. A sketch of the tank and plunger is shown in Figure 2A and a photograph of the same equipment is shown in Figure 2B.

The Porous Media

Polyurethene foam was selected as the porous media to be used in the hydraulic model. It had the advantages of being commercially available and relatively inexpensive; at the same time, it was an elastic material with interconnected pore spaces. Fairly extensive tests were carried out on this material to determine its Young's modulus, its porosity, and the Darcy coefficient of permeability, with the following results:

Young's modulus, $E = 13.6$ psi

Porosity, $\varepsilon = 97$ percent

Darcy permeability, $K = 0.10$ to 0.291 feet/sec.

Specific storage, $S_S = 0.032$ (feet)$^{-1}$

The specific storage is determined from the relation $S_S = w_o\,(1/E + \varepsilon/\beta)$, where the specific weight and the bulk modulus of water have been taken as 62.4 lbs./ft.^{3} and 3.0×10^5 psi, respectively, and E and ε are as above.

The value of the permeability depends on the type of test used. In general, the permeameter test results agree fairly well with the falling-head test results made with the foam in place in a confined condition in the model. A third set of tests, with the foam in place in the model in an unconfined condition, was also made. Both the pressure transducers and a level and point gage were used to measure

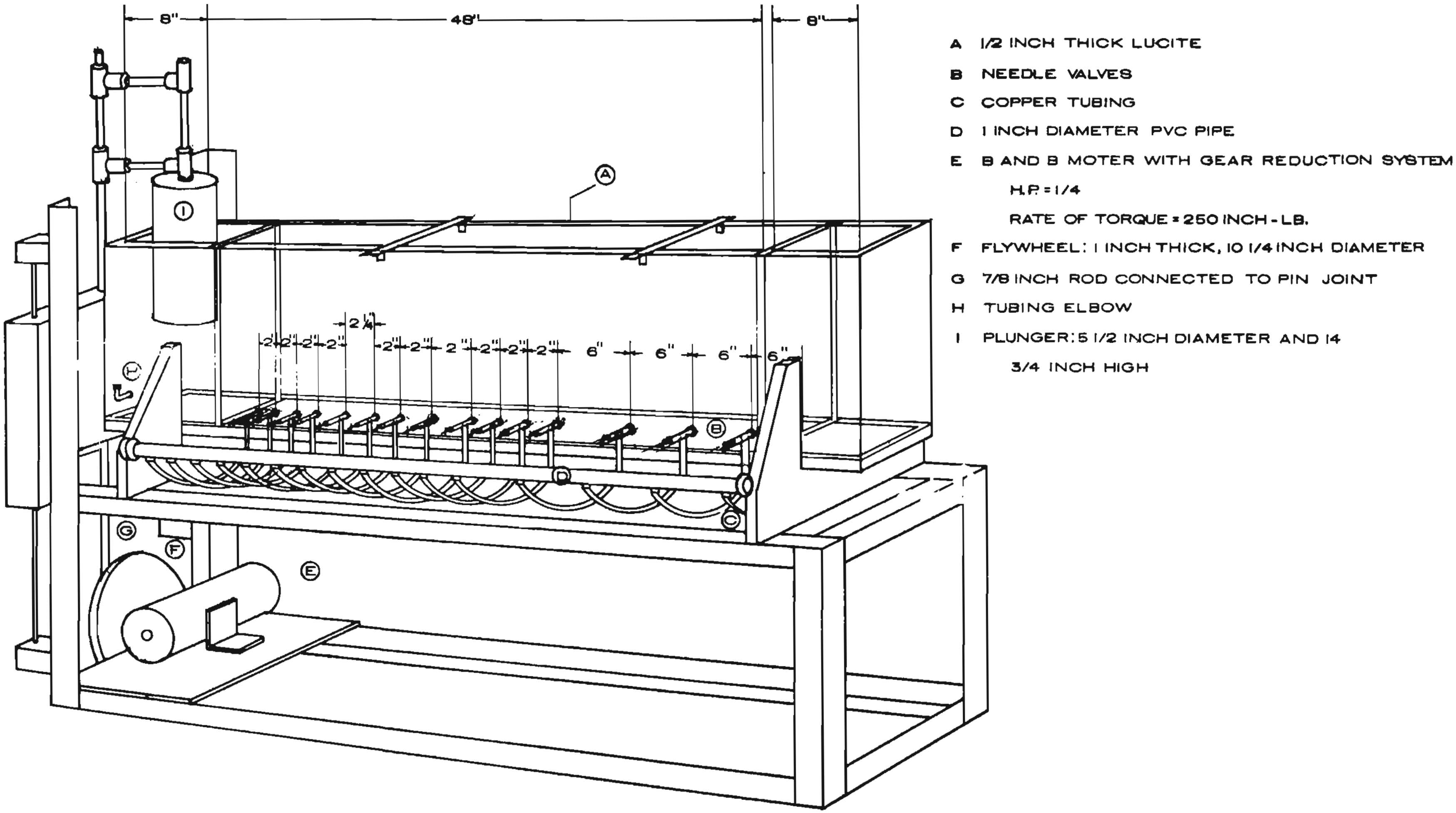

FIGURE 2A. SKETCH OF HYDRAULIC MODEL.

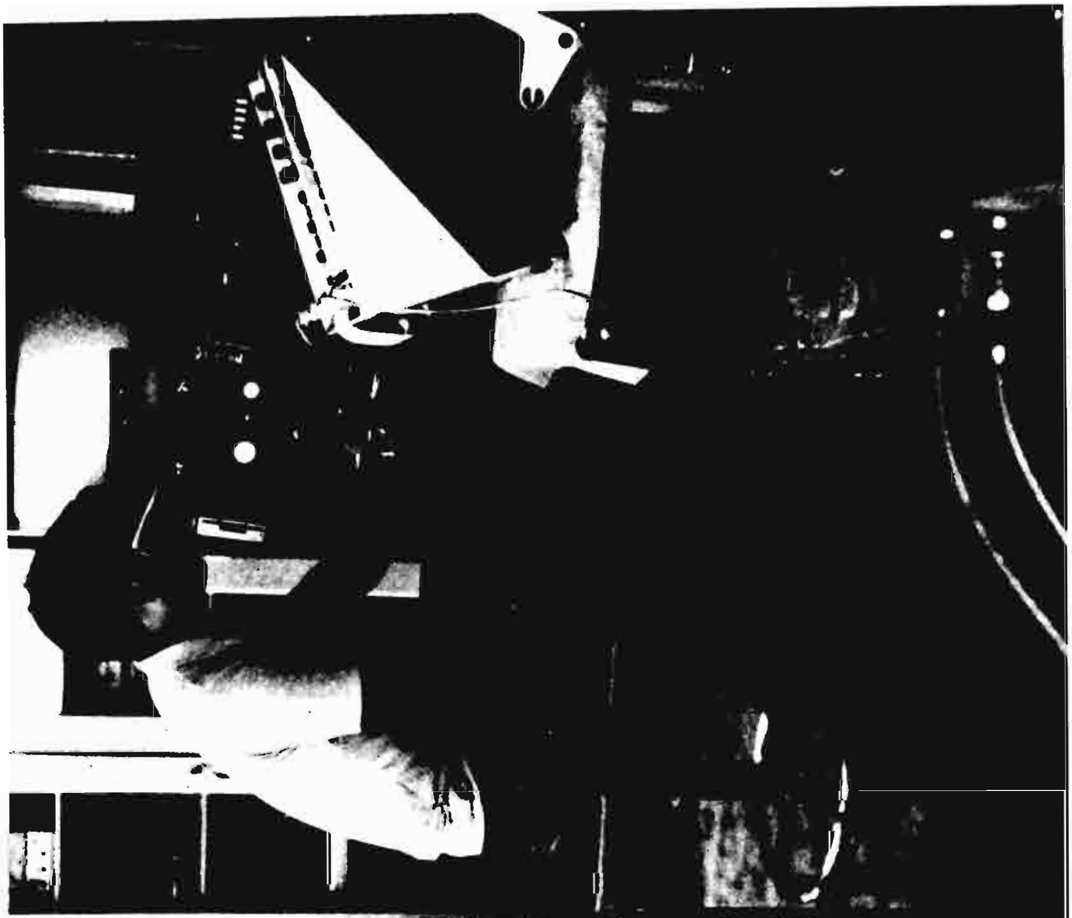

FIGURE 2B. PHOTOGRAPH OF EXPERIMENTAL SET-UP FOR THE HYDRAULIC MODEL.

the water surface elevation directly. The K values resulting from this third set of tests were about 40 percent higher than those of the other tests. Permeameter tests included flows oriented along all three coordinate directions of several foam samples and indicated that the foam was essentially an isotropic material.

A detailed description of the tests and their results are presented in Appendix B.

The Electric Analog Model

The electric analog model consists of a resistance-capacitance network to model the porous media, a Hewlett-Packard model no. 202C or a General Radio model 1310-A audio frequency oscillator to generate the tidal fluctuations, and a direct-current power supply to provide a constant head when that condition was required. A dual-trace oscilloscope, Hewlett-Packard model no. 122A, and a Hewlett-Packard polaroid oscilloscope camera were used to monitor and record both the tidal input at the "coastline" and the corresponding response at any interior point in the network. The resistance-capacitance network is composed of fifty 100-ohm resistors, forty-eight 0.02-microfarad capacitors and two 0.03-microfarad capacitors. All components were rated to be within ±10 percent of their nominal electrical size.

Two different conditions at the internal boundary were simulated: first, the no-flow boundary condition which requires that a reflected disturbance return from the internal boundary; and second, a constant-head boundary condition, i.e., constant voltage, at the internal boundary. The no-flow condition requires that the aquifer be modeled by the first half of the network, while the second half of the network provides an image circuit in which the reflected disturbance can be developed by inserting the same input at both R_{50} and R_1. The constant-head condition can be achieved by placing the DC voltage source in parallel with the resistance-capacitance network at R_{50}, i.e., at the internal boundary.

The circuit diagram for the electric analog model is presented in Figure 3.

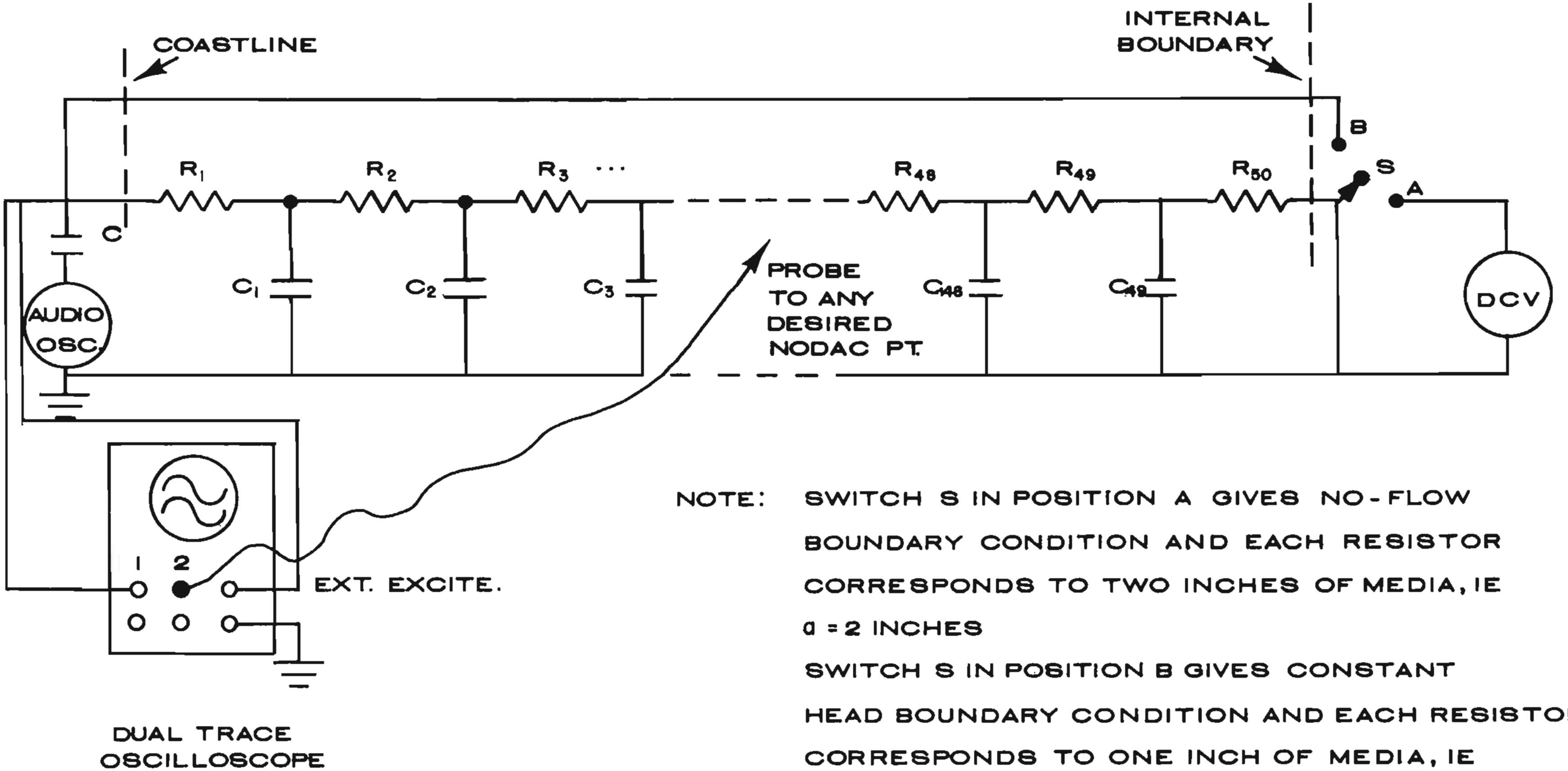

NOTE: SWITCH S IN POSITION A GIVES NO-FLOW BOUNDARY CONDITION AND EACH RESISTOR CORRESPONDS TO TWO INCHES OF MEDIA, IE

$a = 2$ INCHES

SWITCH S IN POSITION B GIVES CONSTANT HEAD BOUNDARY CONDITION AND EACH RESISTOR CORRESPONDS TO ONE INCH OF MEDIA, IE

$a = 1$ INCH.

$R_1 = R_2 = \cdots = R_{50} = 100\,\Omega \pm 10\%$

$C_o = .047\,\mu f \pm 10\%$

$C_1 = C_{49} = .03\,\mu f \pm 10\%$

$C_2 = \cdots = C_{48} = .02\,\mu f \pm 10\%$.

FIGURE 3. SKETCH OF ELECTRIC ANALOG MODEL CIRCUIT.

Experimental Procedure for the Hydraulic Model

The first step was to place the media in the model tank. Three-inch thick strips approximately 0.125 inches wider than the 6-inch tank width were cut to the proper length and placed in the partially-filled model tank. Each strip was then kneaded and squeezed until all the air had been removed.

After positioning the foam in the middle portion of the tank, the procedure varied somewhat, depending on the type of aquifer that was being simulated. If the aquifer was to be confined, the two removable bulkheads were inserted and a polyethylene bag was placed in the region over the media and filled with water. When the water in the end compartments was drained off as the bag filled, the foam layers compressed and the bag seated itself around the edges of the foam. Once the bag was seated, the water level in the tidal compartment was raised until the level at high tide was about one inch below the level of the water in the plastic bag, thus keeping an excess pressure in the region over the foam. The excess pressure kept the bag seated and leakage into the region between the bag, foam, and lucite wall was minimized. The bulkhead, representing the internal boundary, was positioned with its lower edge coincident with the tank bottom if the no-flow boundary condition was required, and with its lower edge coincident with the upper surface of the foam layers if the constant-head boundary condition was required. For the latter condition, the water flowed through the media from the tidal compartment until there was no head difference between the two ends of the media. This zero-head difference represented the equilibrium condition about which the tidal fluctuations occurred. The bulkhead, partitioning off the coastal end of the aquifer, was positioned with its lower edge coincident with the upper surface of the porous media.

For an unconfined aquifer with constant-head boundary condition, neither the bulkheads nor the plastic bag were required. The no-flow boundary condition was achieved, as before, by inserting a bulkhead at the internal boundary.

The remaining steps in the procedure were the same for both types of aquifers. The desired equilibrium level in the model was established and all the air bled from the manifold and the lines leading to the transducers. A tidal period and amplitude were selected and the tidal generator turned on. A continuous history of the tidal change was recorded on one channel of the recorder while the corresponding fluctuation in piezometric head at the several pressure taps located in the media was recorded on the second channel. These fluctuations were recorded every six inches, by leaving the appropriate needle valve open for several tidal periods and then closing it.

A summary of the test conditions used with the hydraulic model is presented in Table 1, and a sample record for tests of KONA for September 1969 is shown in Figure 4A.

TABLE 1. SUMMARY OF EXPERIMENTAL CONDITIONS, HYDRAULIC MODEL.

DATE OF EXPERIMENT	TYPE OF AQUIFER	AQUIFER DIMENSIONS, IN.		AVG. WATER DEPTH, IN., AT X = L	TIDAL CHANGE, IN.	TIDAL PERIOD, SEC.	Δh AT X = 0, IN.
		L	b				
17 AUG.	POHA	48	12.00	10.375	2.1	12, 9, 6, 3	.25, .13, .07, 0
17 AUG	PONO	48	12.00	10.375	2.1	12, 9, 6, 3	--
18 AUG.	POHA	48	6.00	5.436	0.5	9, 6, 3	.05, .03, 0
18 AUG.	PONO	48	6.00	5.436	0.5	9, 6, 3	--
20 AUG.	KOHA	50	2.875	14.75	3.0	12, 9, 6, 3	?
23 AUG.	KONA	50	2.875	14.75	3.0	12, 9, 6, 3, 1.5	--
3 SEPT.	KOHA	50	5.875	15.312	1.0	12, 6, 3, 1.5	.08, .03, 0, 0
4 SEPT.	KONA	50	5.875	16.436	1.0	12, 9, 6, 3, 1.5	--
9 SEPT.	PONO	49	6.00	5.250	0.65	9, 6, 3, 1.5	--
9 SEPT.	POHA	49	6.00	5.250	0.65	9, 6, 3, 1.5	.04, .03, 0, 0
10 SEPT.	PONO	49	6.00	5.250	0.32	6, 3, 1.5	--

Experimental Procedure for the Electric Analog Model

The first step in the procedure was to determine the time scale factor, K_4. This required selecting the appropriate value for the Darcy permeability and the desired boundary condition. The selection of the appropriate value of K is discussed in "Analysis and Presentation of the Data" (p.22) and Appendix C contains sample calculations for K_4 for the tests on KONA for 4 September 1969. With K_4 established, the audio oscillator was set at the appropriate frequency. Switch, S, was placed in a position consistent with the boundary condition required, and the oscilloscope turned on. Trace 1 on the oscilloscope always recorded the input wave form while Trace 2 gave the response to this input at

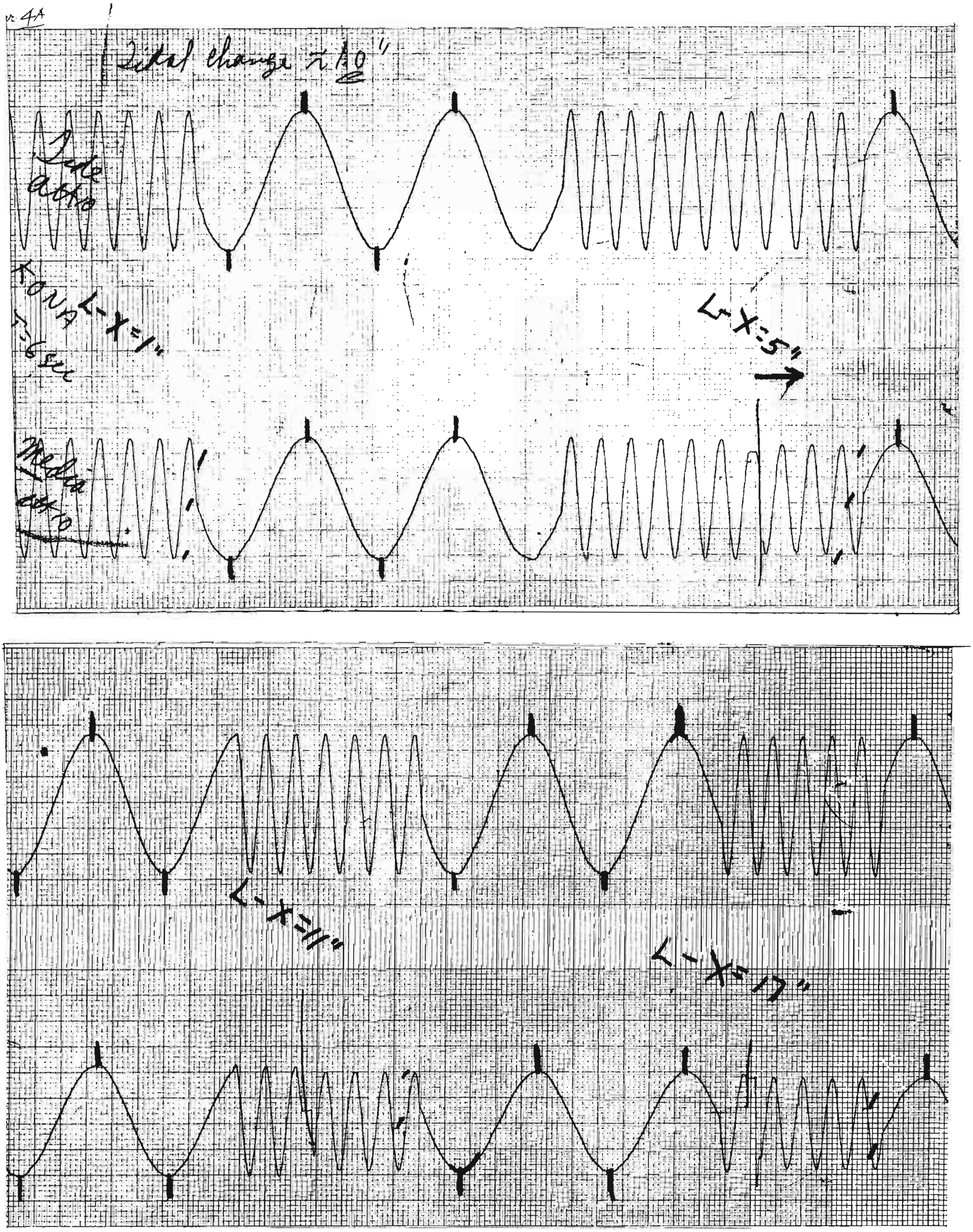

FIGURE 4A. RECORDS FROM HYDRAULIC MODEL, TESTS OF KONA, 4 SEPT. 1969.

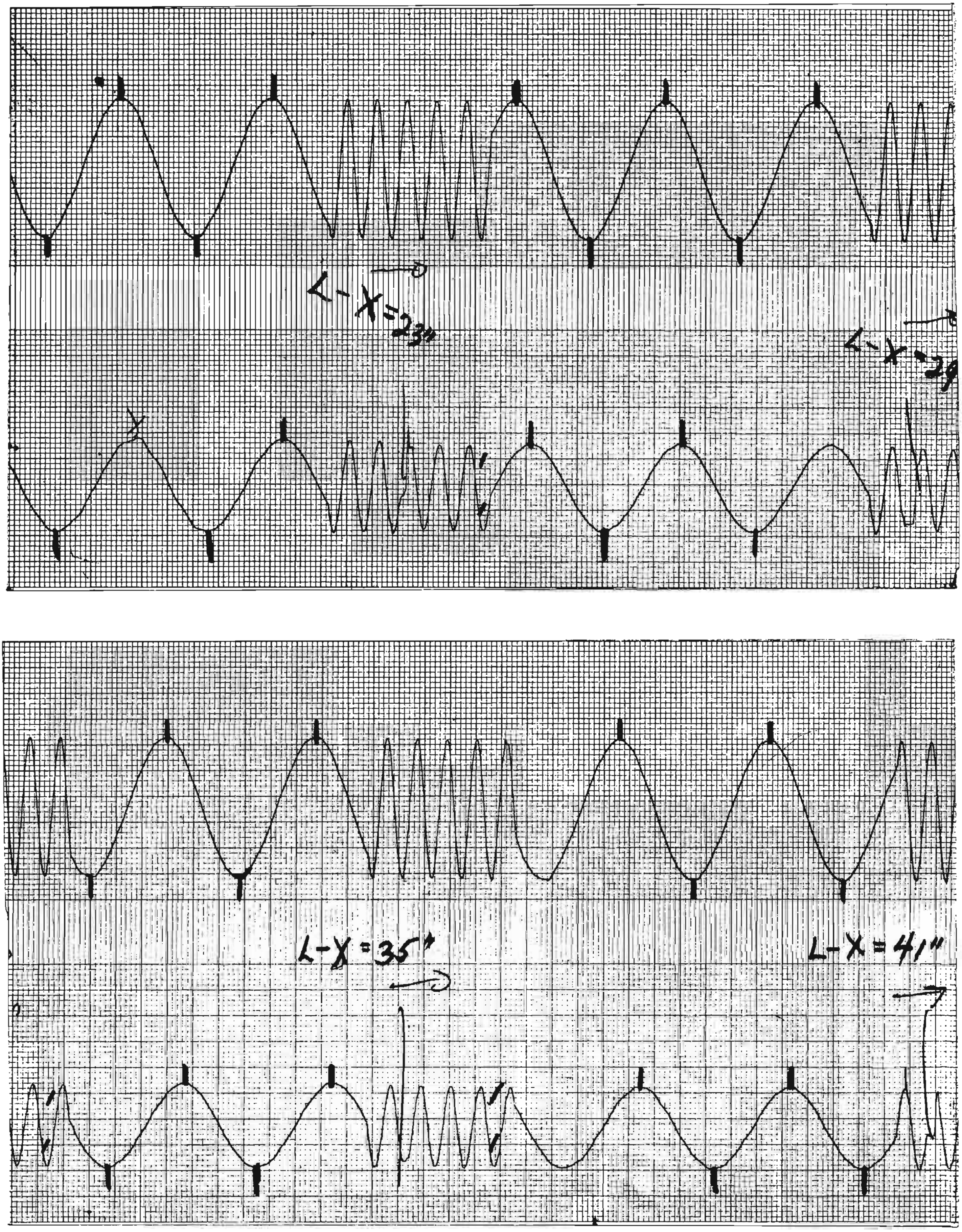

FIGURE 4A (CONT'D).

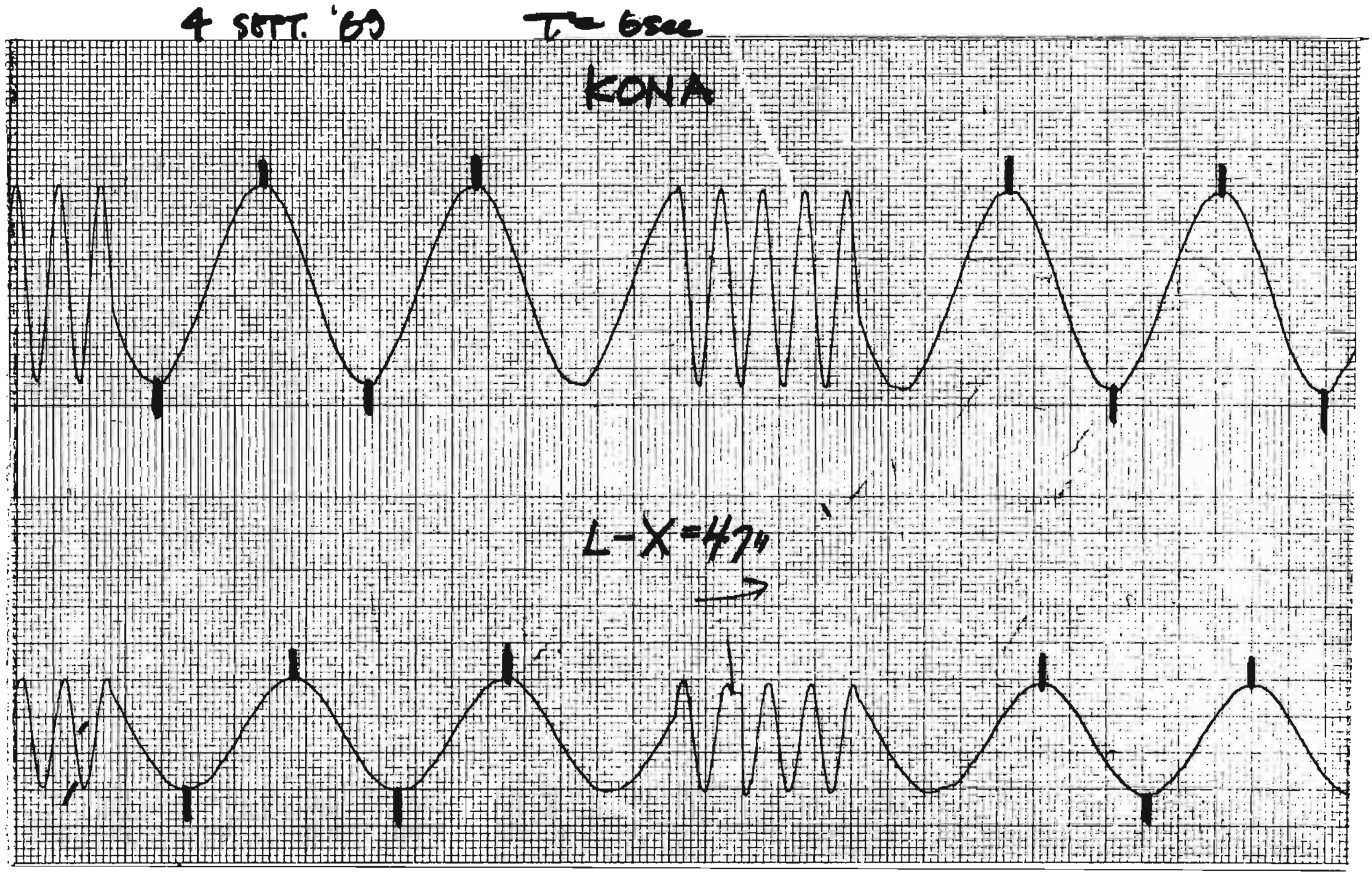

FIGURE 4A (CONT'D).

any interior point where the oscilloscope probe was applied. The response was measured at those points corresponding to the six-inch intervals used in the hydraulic model. For the no-flow boundary condition, this interval is 300 ohms (i.e., a = 2 inches) and for the constant-head boundary condition, it is 600 ohms (i.e., a = 1 inch). At each position a photograph of the input and the response was made. As the film was exposed only to the illuminated portion of the cathode ray tube, Trace 2 at all eight positions was photographed on a single Polaroid film by simply using the vertical adjustment control to reposition the trace on the cathode ray tube for each new position of the probe. Since the input remained constant, it was eliminated from all but the first exposure.

Table 2 summarizes the conditions of the tests with the electric analog model and Figure 4B presents a photograph of the wave forms observed for the test conditions on KONA for 4 September 1969.

TABLE 2. SUMMARY OF EXPERIMENTAL CONDITIONS, ELECTRIC ANALOG.

DATE OF EXPERIMENT	TYPE OF AQUIFER	CONSTANT VOLTAGE DC VOLTS	CHANGE IN VOLTAGE VOLTS	ELECTRIC ANALOG FREQUENCY IN CPS/AVG. DARCY COEFFICIENT OF PERMEABILITY FT/SEC.				
				12 SEC.	9 SEC.	6 SEC.	3 SEC.	1.5 SEC.
17 AUG.	POHA	12.5	0.6	92 3.59	101 4.27	125 5.20	173 7.53	
17 AUG.	PONO	0	0.6	133 9.66	184 9.33	253 10.15	501 10.24	
18 AUG.	POHA	12.5	0.6		122 7.5	160 7.2	250 13.5	
18 AUG.	PONO	0	0.6		229 14.3	312 15.7	663 14.8	
20 AUG.	KOHA	12.5	0.6		311 0.039	344 0.053	520 0.070	
23 AUG.	KONA	0	0.7	810 0.045	1080 0.045	1620 0.045	3240 0.045	
3 SEPT.	KOHA	12.5	0.6	61 0.15		114 0.16	227 0.16	404 0.18
4 SEPT.	KONA	0	0.6	204 0.18	244 0.20	348 0.21	536 0.25	1172 0.25
9 SEPT.	PONO	0	0.6		331 10.32	384 13.35	680 15.10	1257 16.35
9 SEPT.	POHA	12.5	0.6		111 7.7	144 8.9	182 14.1	330 15.5
10 SEPT.	PONO	0	0.6			395 13.0	790 13.0	1630 12.6

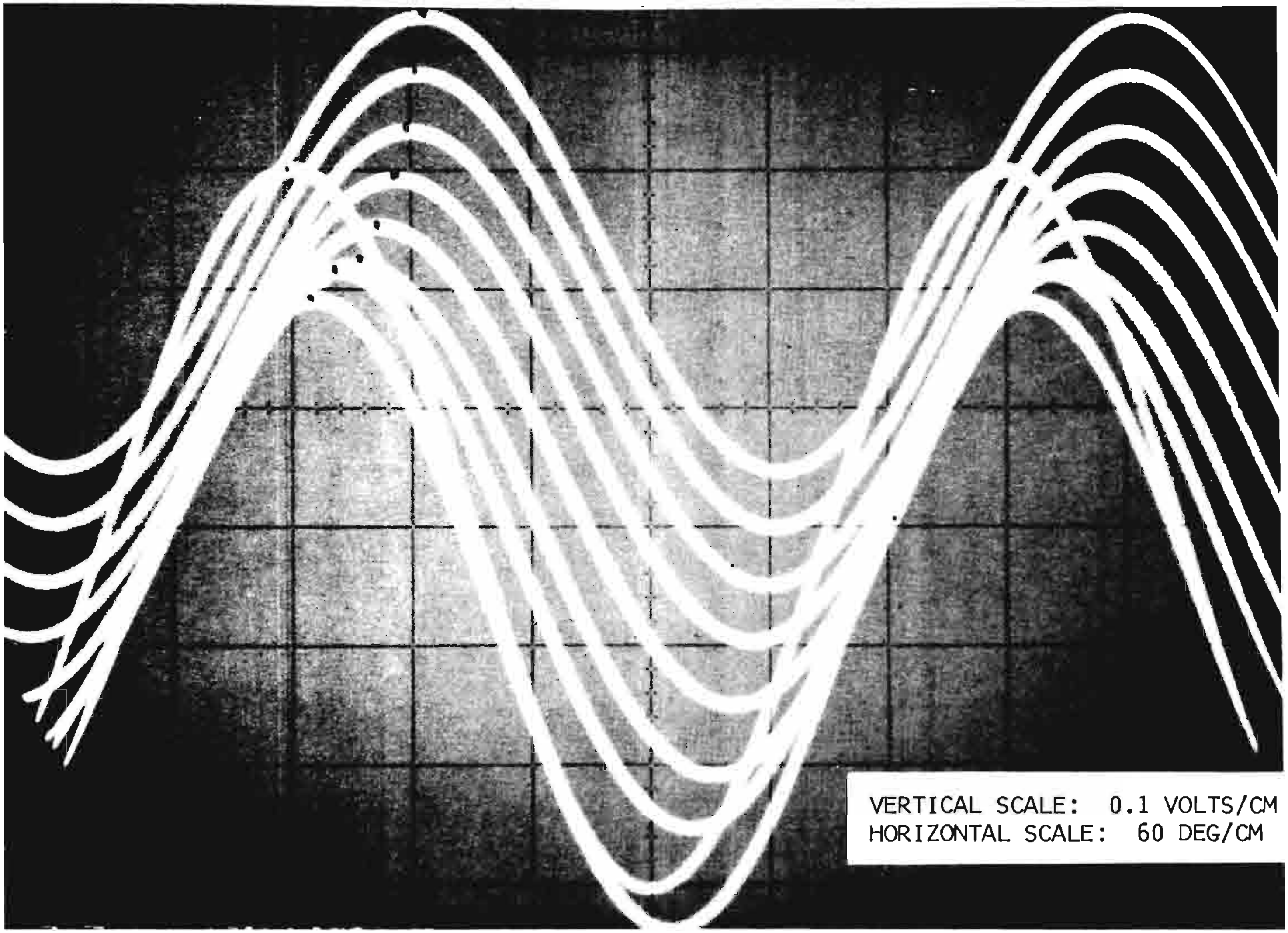

FIGURE 4B. PHOTOGRAPH OF WAVE FORMS FROM ELECTRIC ANALOG, TESTS OF KONA, 4 SEPT. 1969.

ANALYSIS AND PRESENTATION OF THE DATA

The Hydraulic Model Data

Analyzing the data from the hydraulic model tests required that amplitude and phase angles be determined from the time histories of the piezometric surface similar to those shown in Figure 4A. To facilitate the presentation of the data, all amplitudes were normalized with respect to the amplitude of the fluctuation at the coastline, i.e., the tidal amplitude. Since the recorder response was linear with respect to the changes in the piezometric surface, this normalization was accomplished by dividing the number of chart lines from peak to trough for each record taken by the number of chart lines from peak to trough counted on the same channel from the time history recorded nearest to the coastline. The latter time history was not always recorded exactly at $x = L$, but was always close enough to $x = L$ so that differences in the amplitudes were less than those small differences occurring randomly in the generated tidal change, i.e., less than 2 percent. The number of lines used in each case was taken as the average number of chart lines based on three consecutive waves.

Phase angles were determined by projecting the peaks and troughs of the trace recording fluctuations in the media into the trace recording the tidal change. The phase angle was then measured as the distance between the projected peak or trough and the peak or trough of the tidal trace. The appropriate peaks or troughs were not difficult to identify as the phase angles increased slowly from zero with distance from the coastline. The accuracy with which these angles could be scaled off depended on the chart speed and the wave period. This scale factor varied from 12°/mm, which corresponds to a 1.5 second period tide and a 20-mm/sec. chart speed, to 6°/mm which corresponds to a 12-second period tide and a 5-mm/sec. chart speed.

As the amplitude decreased the peaks and troughs flattened out, making it difficult to pick out the maximum and minimum points. This effect was minimized by increasing the sensitivity of the recorder for several cycles of the tide whenever the crest-to-trough distance became less than six or eight lines.

For the longer periods, the torque on the tidal-generator motor was not constant and produced a tidal change which was not strictly sinusoidal, but contained some higher harmonics. This resulted in two different values for the phase angle, since the phase shift for the crests was not the same as that for the troughs. However, the effect was eliminated by averaging the two values of the phase angle. Both the phase angle calculated from the crest shifts and that calculated from the trough shifts were average values based on three successive cycles of the two traces.

Plots of the normalized amplitude, ρ, and the phase angle, Θ_p, as functions of the normalized distance from the coastline, x/L, are presented in Figures 5 through 15. The hydraulic model data is represented by the unshaded symbols.

Determination of K from Hydraulic Model Data

In order to determine the Darcy permeability from an amplitude decay curve, values of ρ were scaled off the plots of ρ vs x/L at points corresponding approximately to x/L = 0.75, 0.50, 0.25, and 0.04. Each pair of values of ρ and x/L was substituted into the appropriate equation for ρ given in the section on "The Mathematical Model" (p. 2). The equation was then solved for α by employing the Newton-Rhapson technique for determining the roots of an equation and the IBM 360 computer. K could then be calculated since it was the only unknown factor in α. A sample program employing the data of KONA, 4 September 1969, is presented in Appendix D. The K values thus determined are plotted as functions of x/L and are presented in Figures 16, 17, and 18. From these plots, an average value of the Darcy permeability was estimated for each tidal period tested. These average values of permeability are given in Table 2.

The Newton-Rhapson method failed when applied to some of the data obtained from the POHA models. The reason for this is the nearly linear decay of the amplitudes (see Figs. 13 and 15). Equation (5a) relating ρ and x may be rewritten as

$$\rho = x\left[(1 + \frac{\alpha^2}{90}x^4 + \cdot\cdot\cdot)/(1 + \frac{\alpha^2}{90} + \cdot\cdot\cdot)\right]^{1/2} .$$

The quantity in brackets must approach unity if the amplitude decay ap-

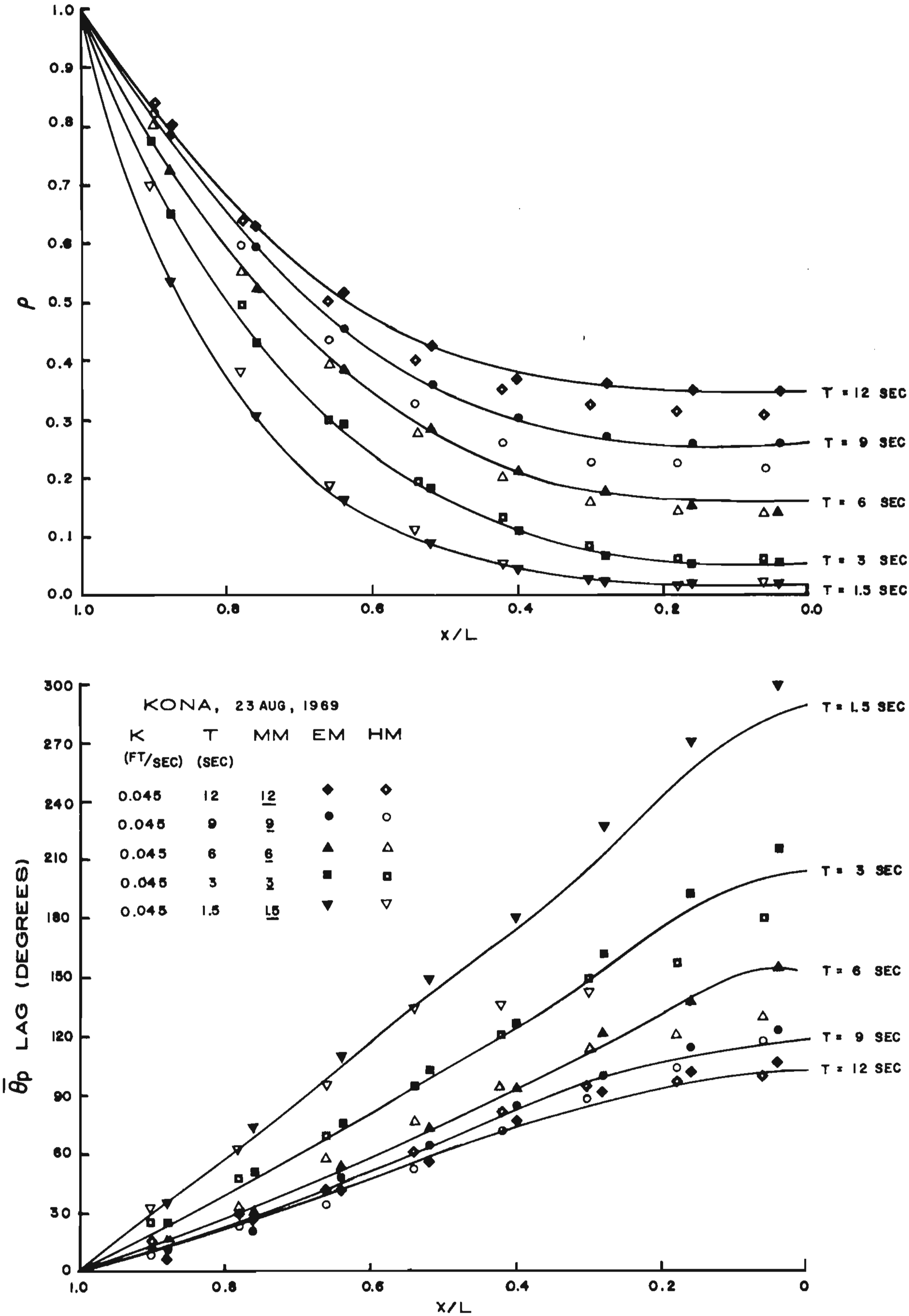

FIGURE 5. AMPLITUDE AND PHASE ANGLE VS x/L
FOR KONA, 23 AUG. 1969 DATA.

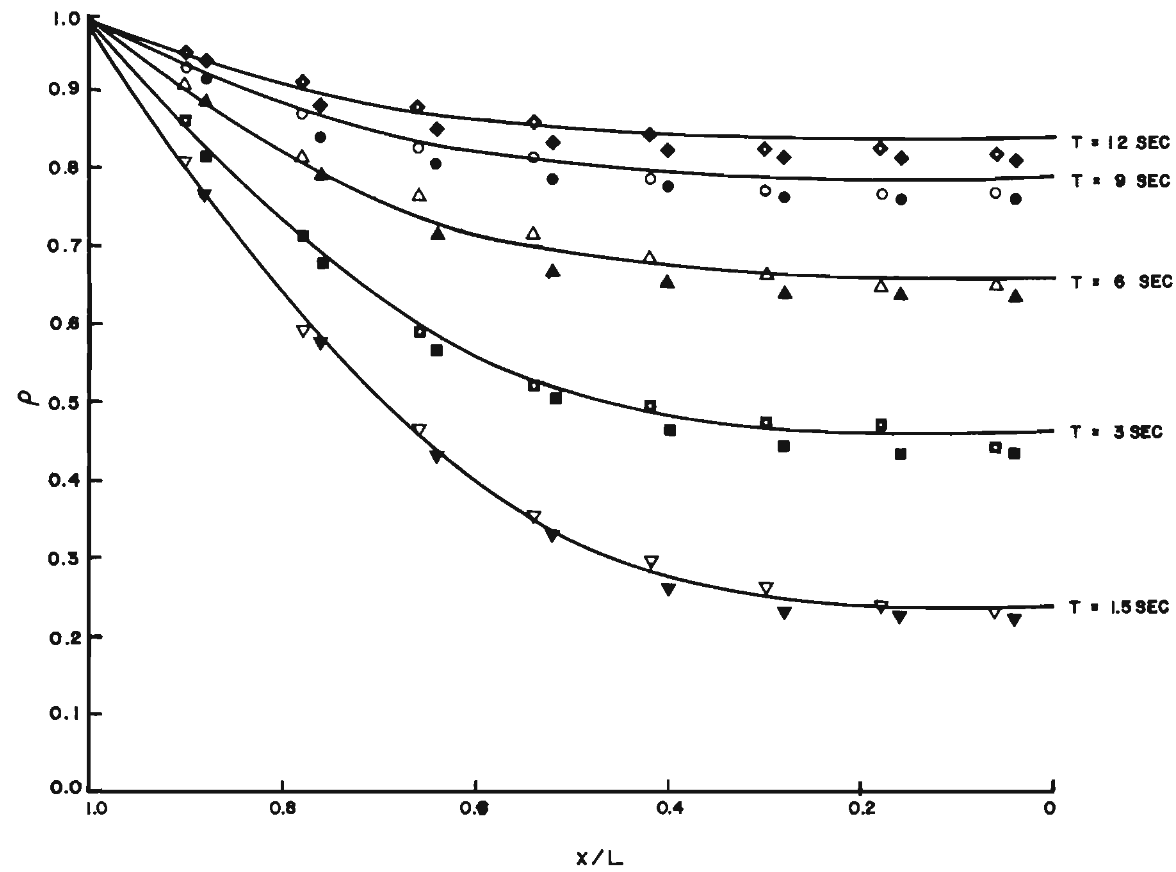

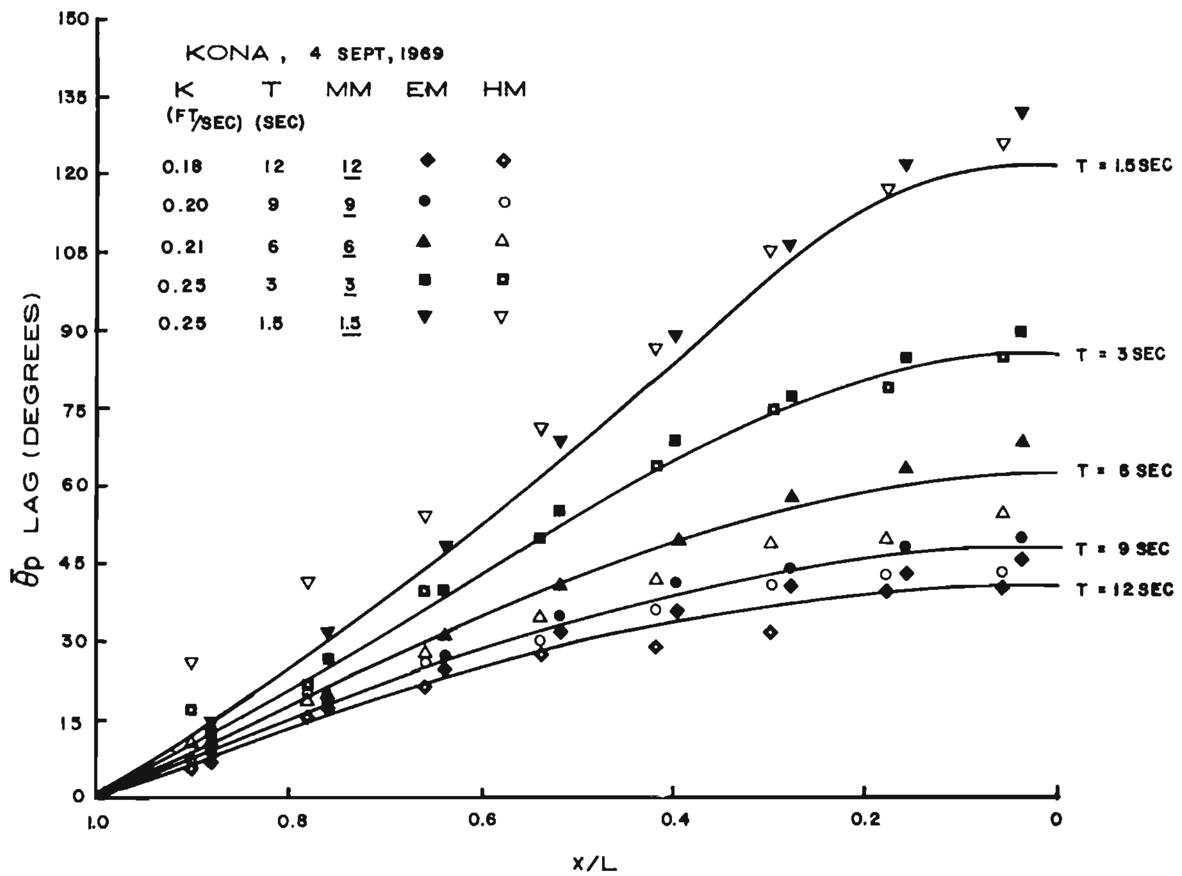

FIGURE 6. AMPLITUDE AND PHASE ANGLE VS x/L
FOR KONA, 4 SEPT. 1969 DATA.

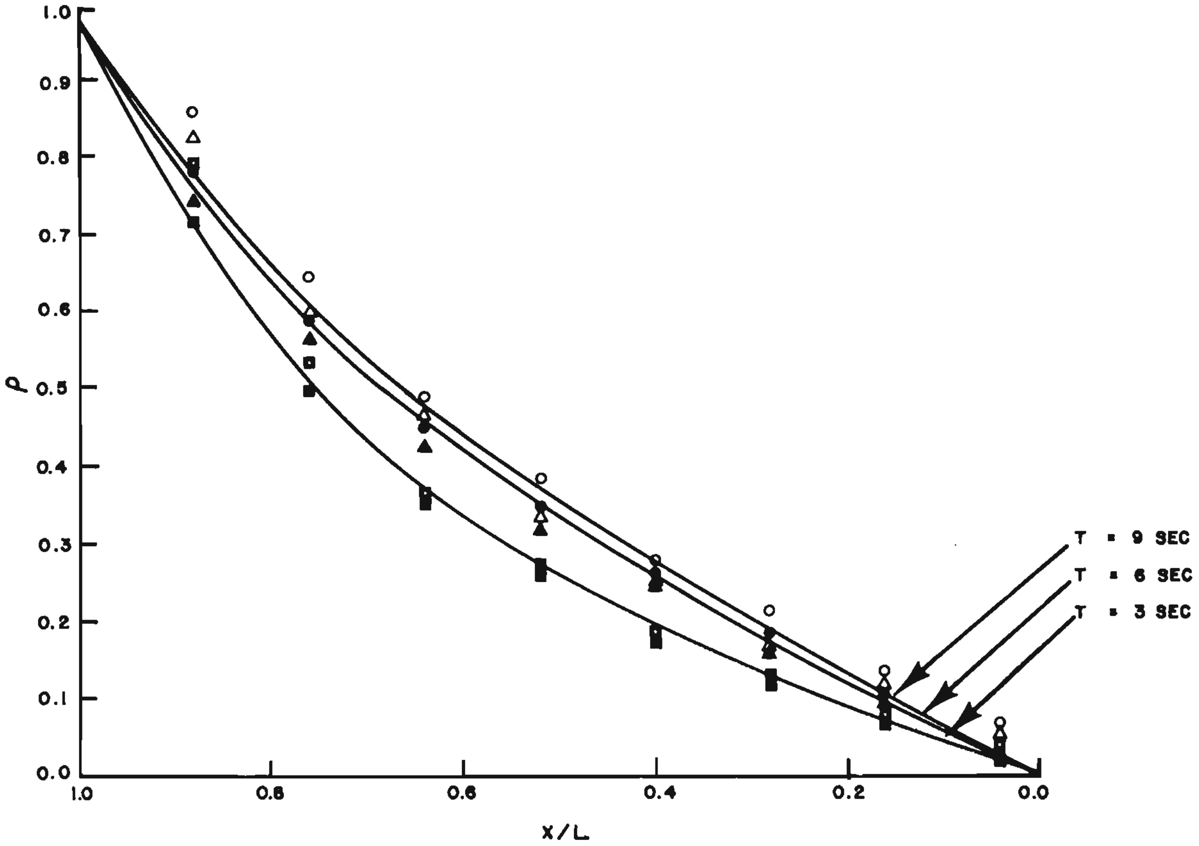

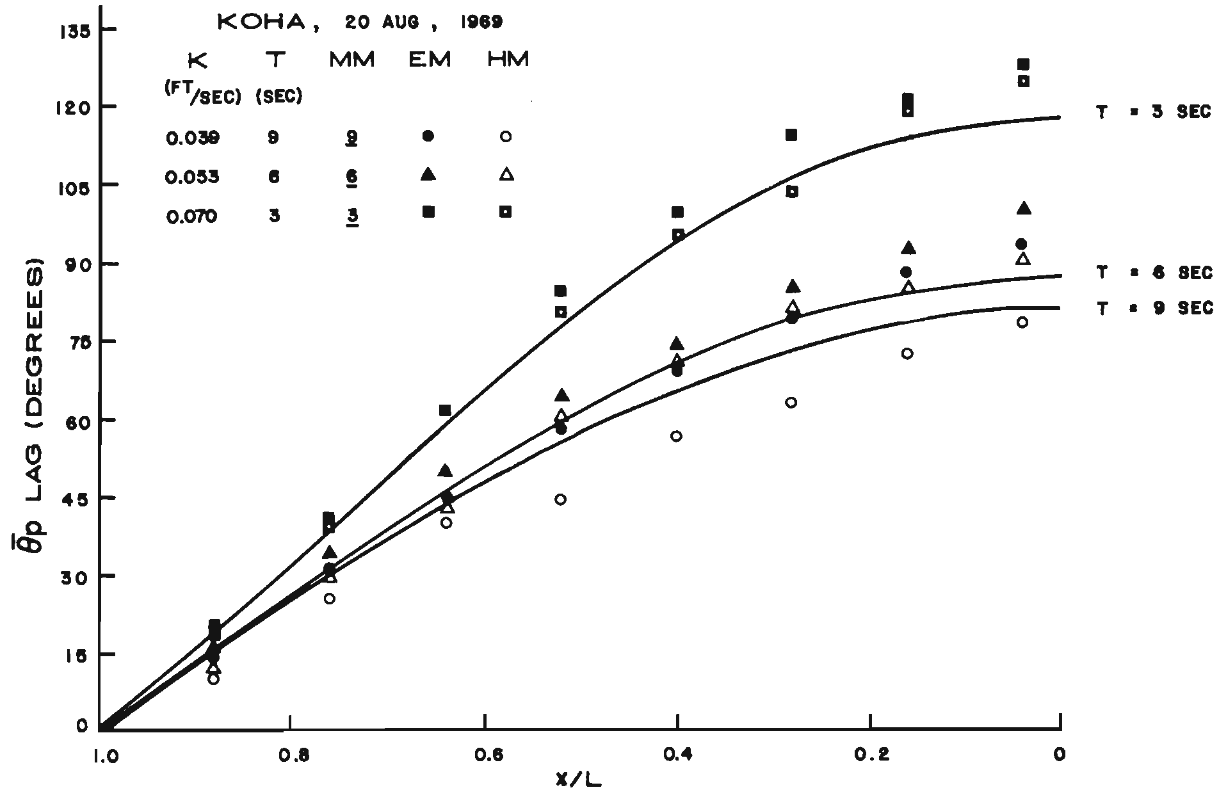

FIGURE 7. AMPLITUDE AND PHASE ANGLE VS x/L FOR KOHA, 20 AUG. 1969 DATA.

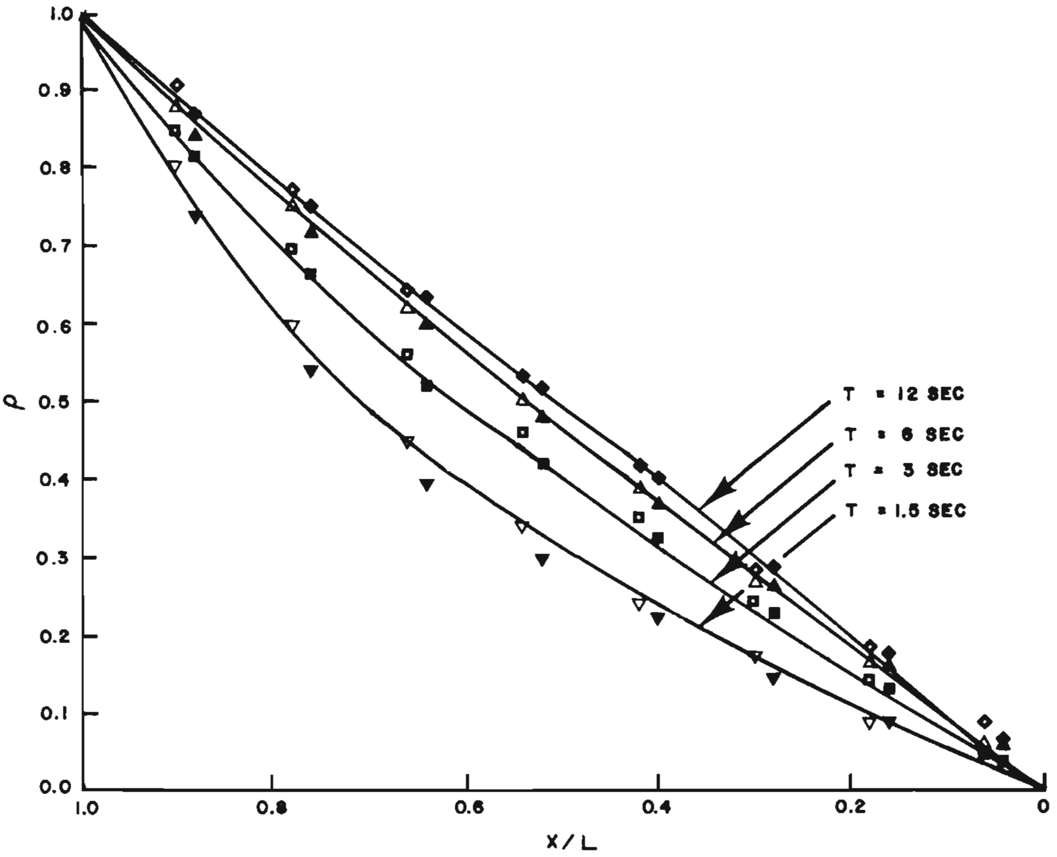

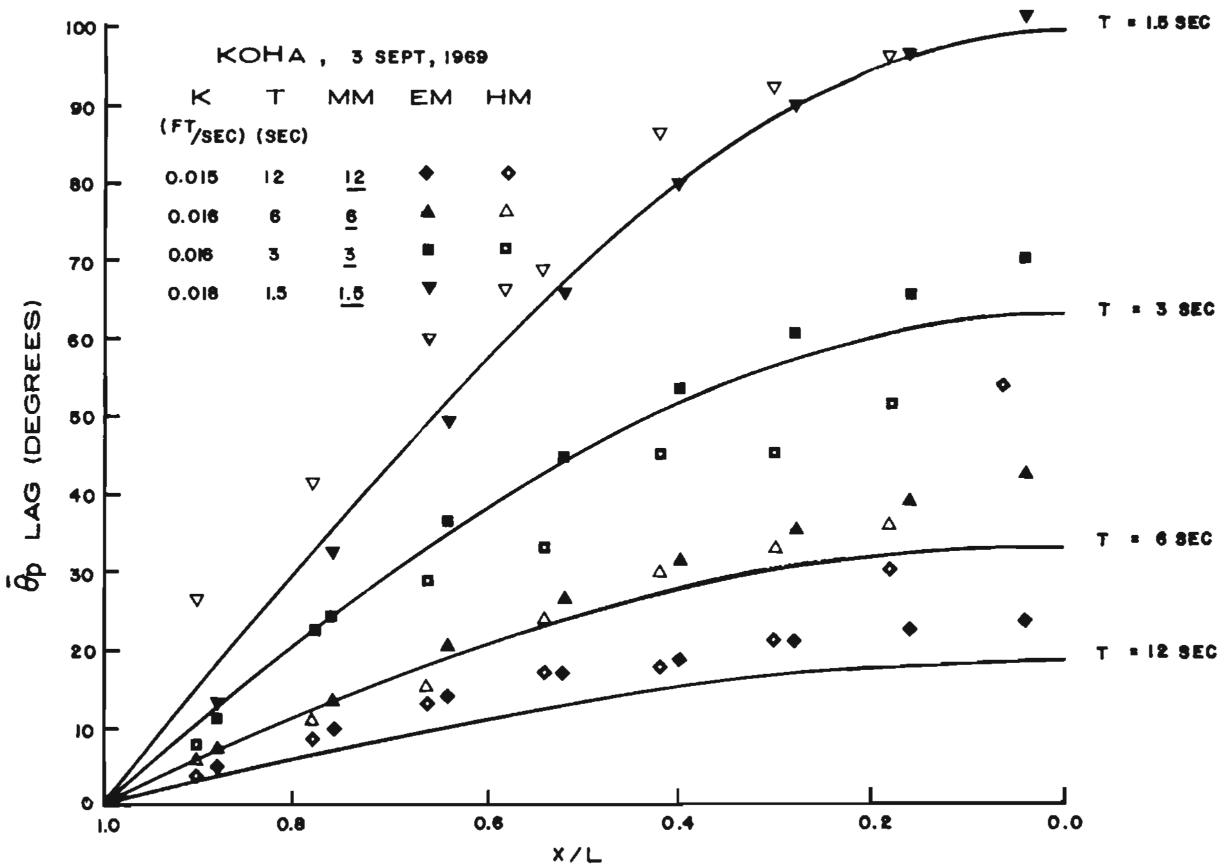

FIGURE 8. AMPLITUDE AND PHASE ANGLE VS x/L
FOR KOHA, 3 SEPT. 1969 DATA.

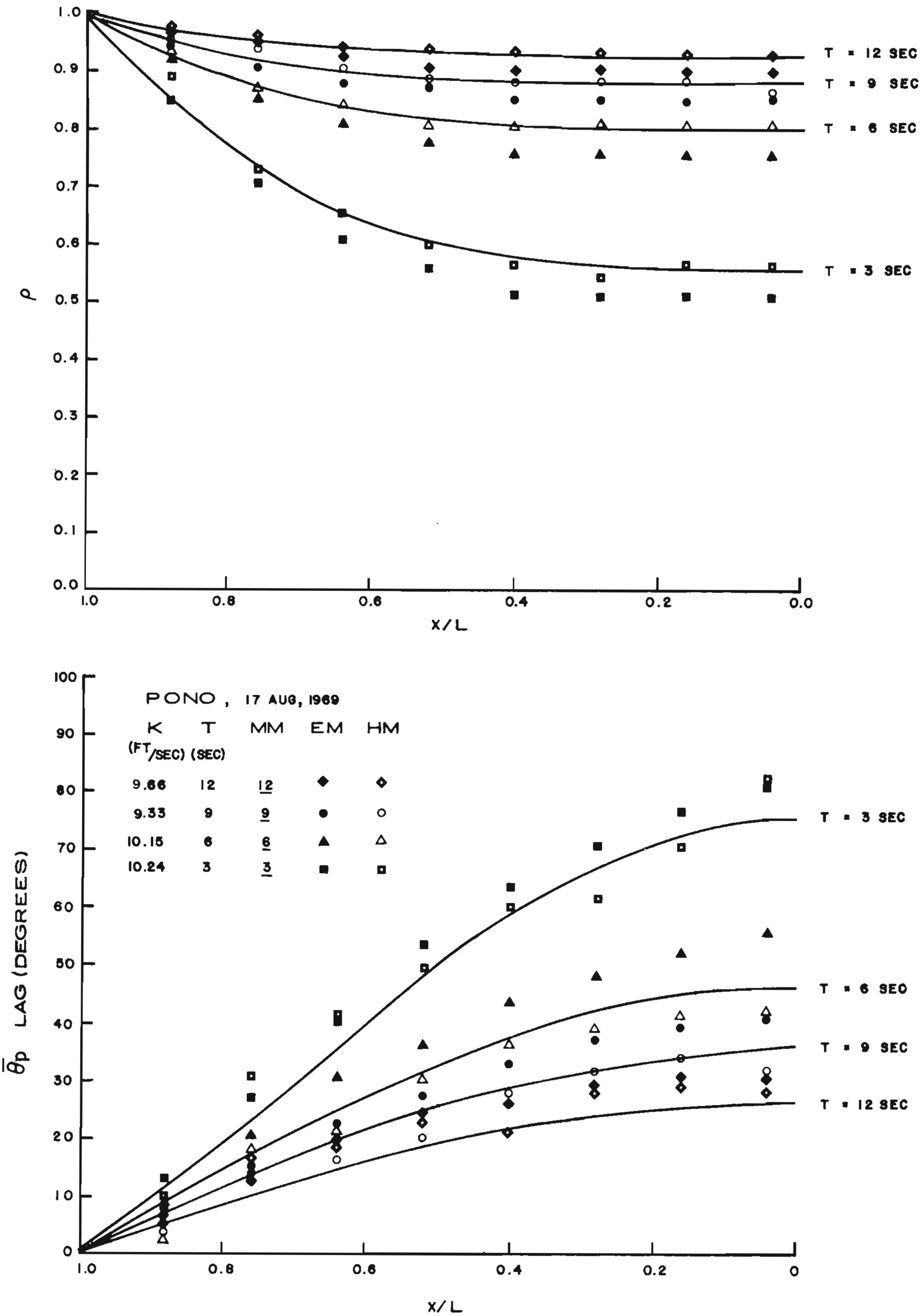

FIGURE 9. AMPLITUDE AND PHASE ANGLE VS x/L FOR PONO, 17 AUG. 1969 DATA.

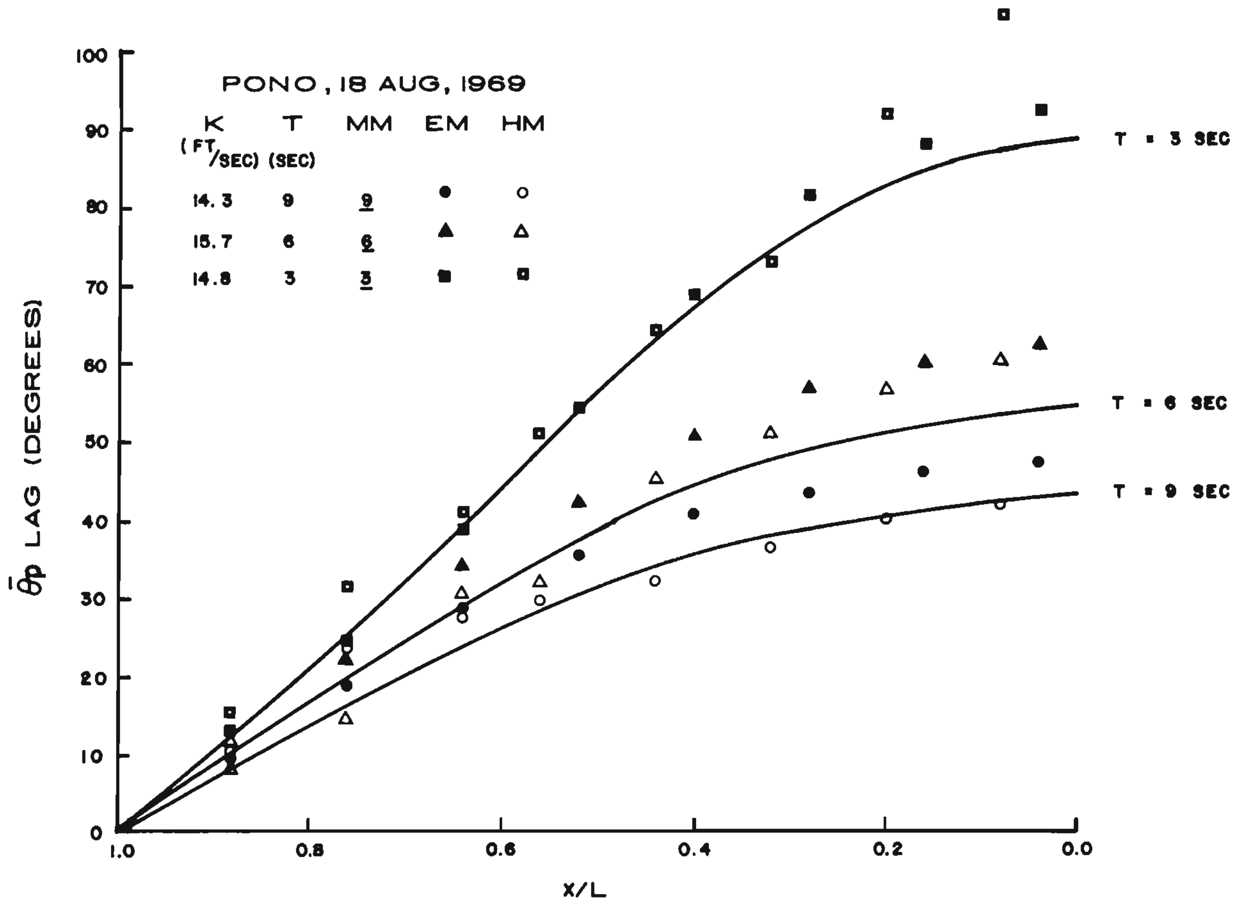

FIGURE 10. AMPLITUDE AND PHASE ANGLE VS x/L
FOR PONO, 18 AUG. 1969 DATA.

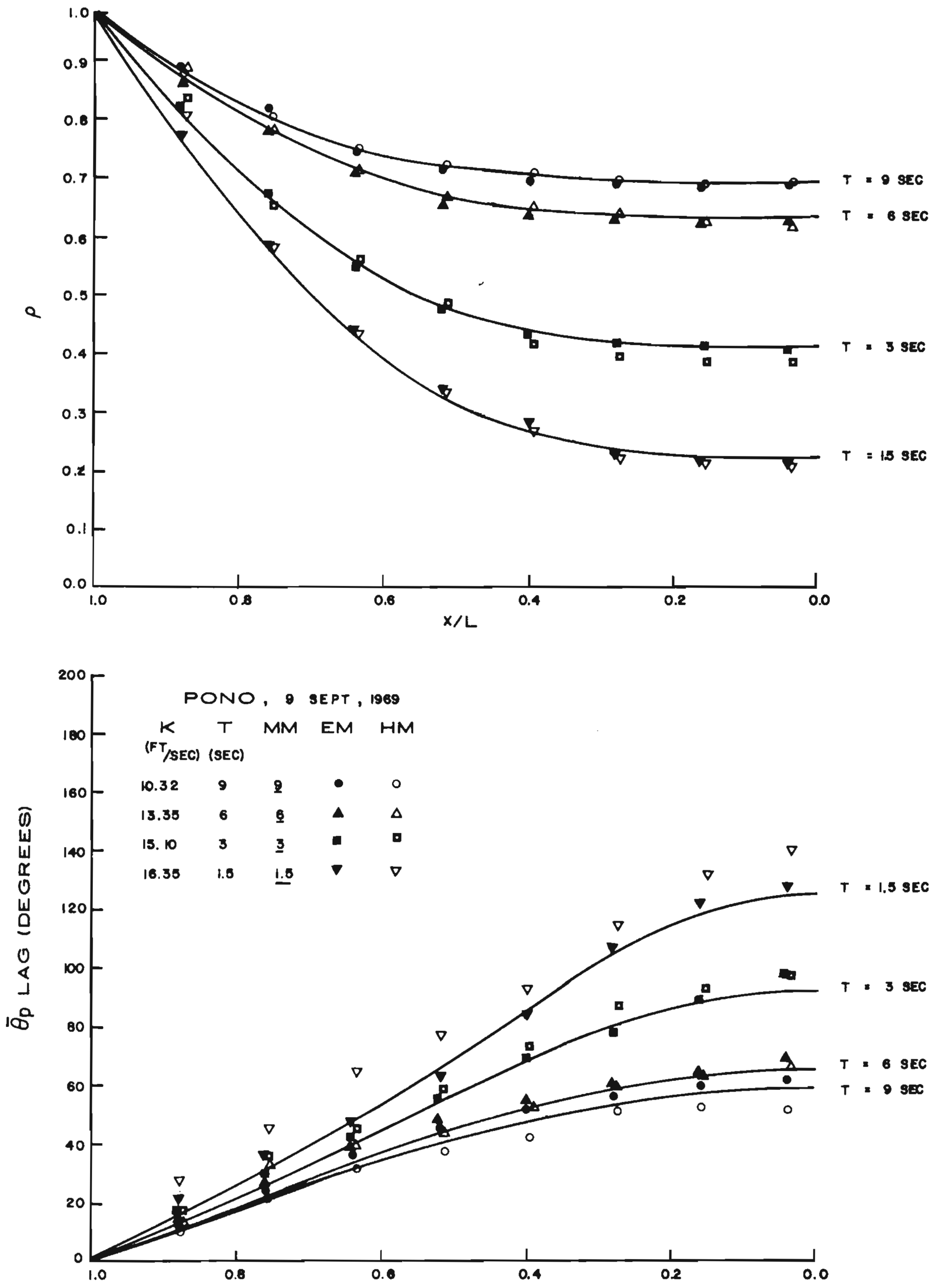

FIGURE 11. AMPLITUDE AND PHASE ANGLE VS x/L FOR PONO, 9 SEPT. 1969 DATA.

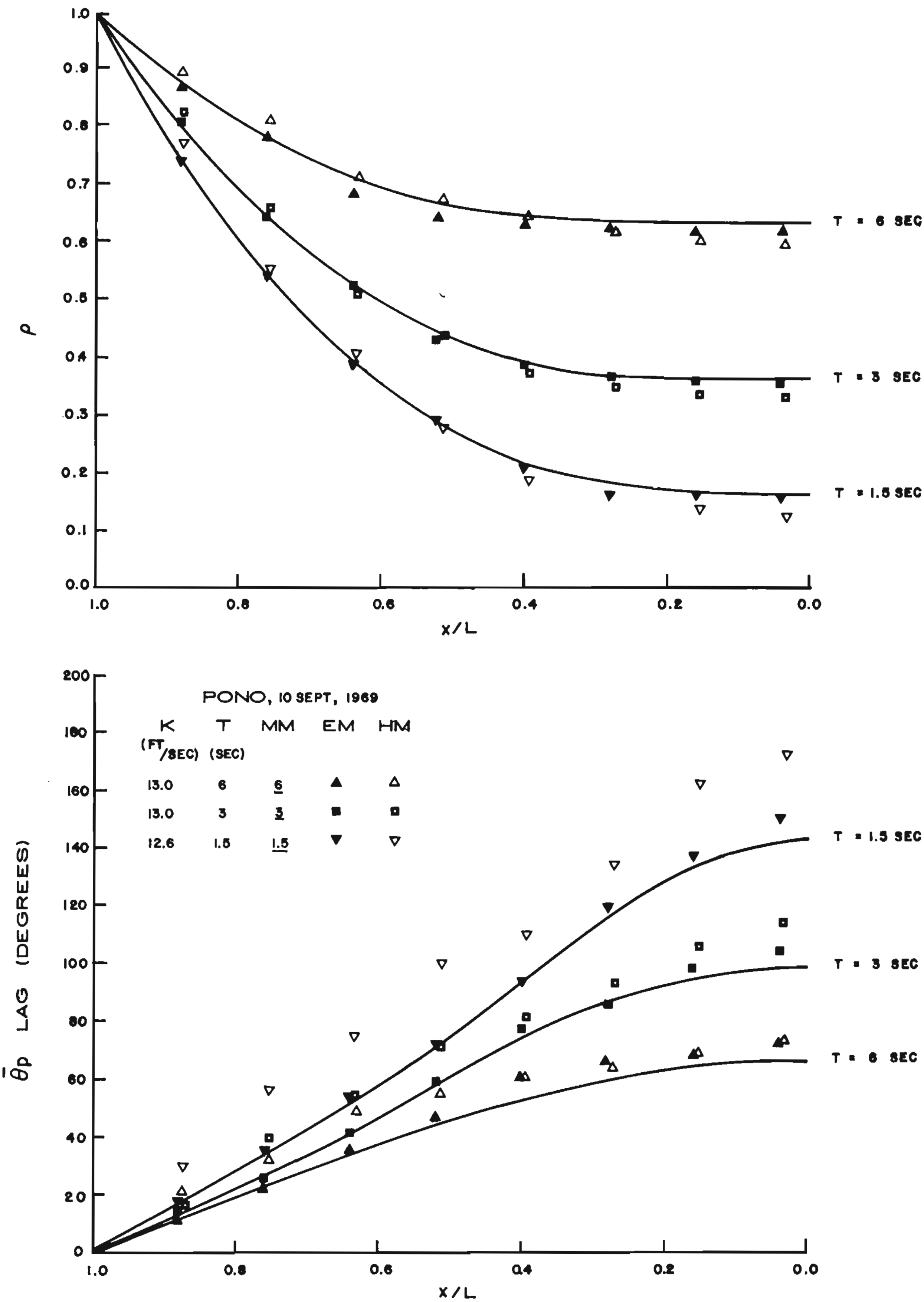

FIGURE 12. AMPLITUDE AND PHASE ANGLE VS x/L FOR PONO, 10 SEPT. 1969 DATA.

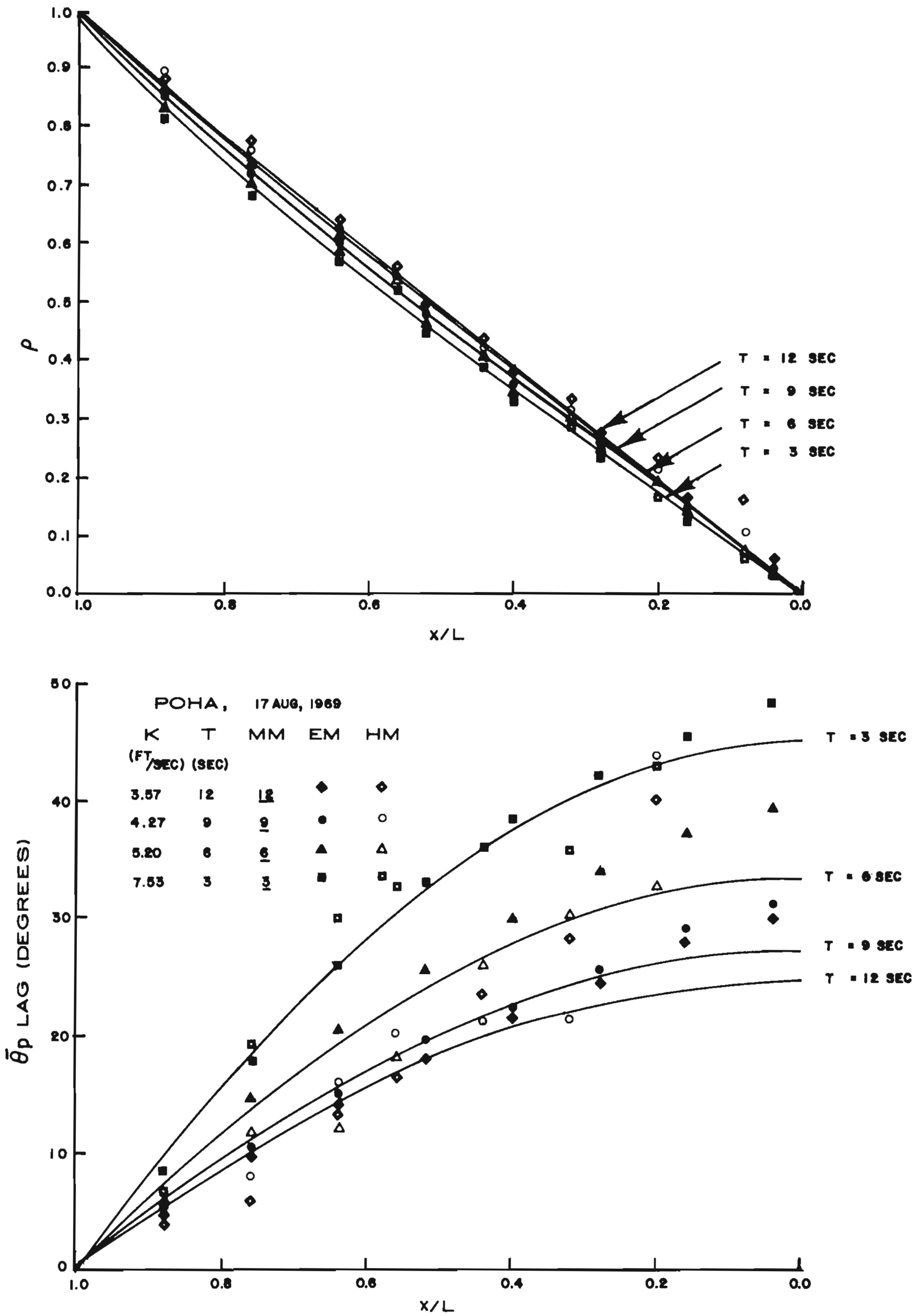

FIGURE 13. AMPLITUDE AND PHASE ANGLE VS x/L
FOR POHA, 17 AUG. 1969 DATA.

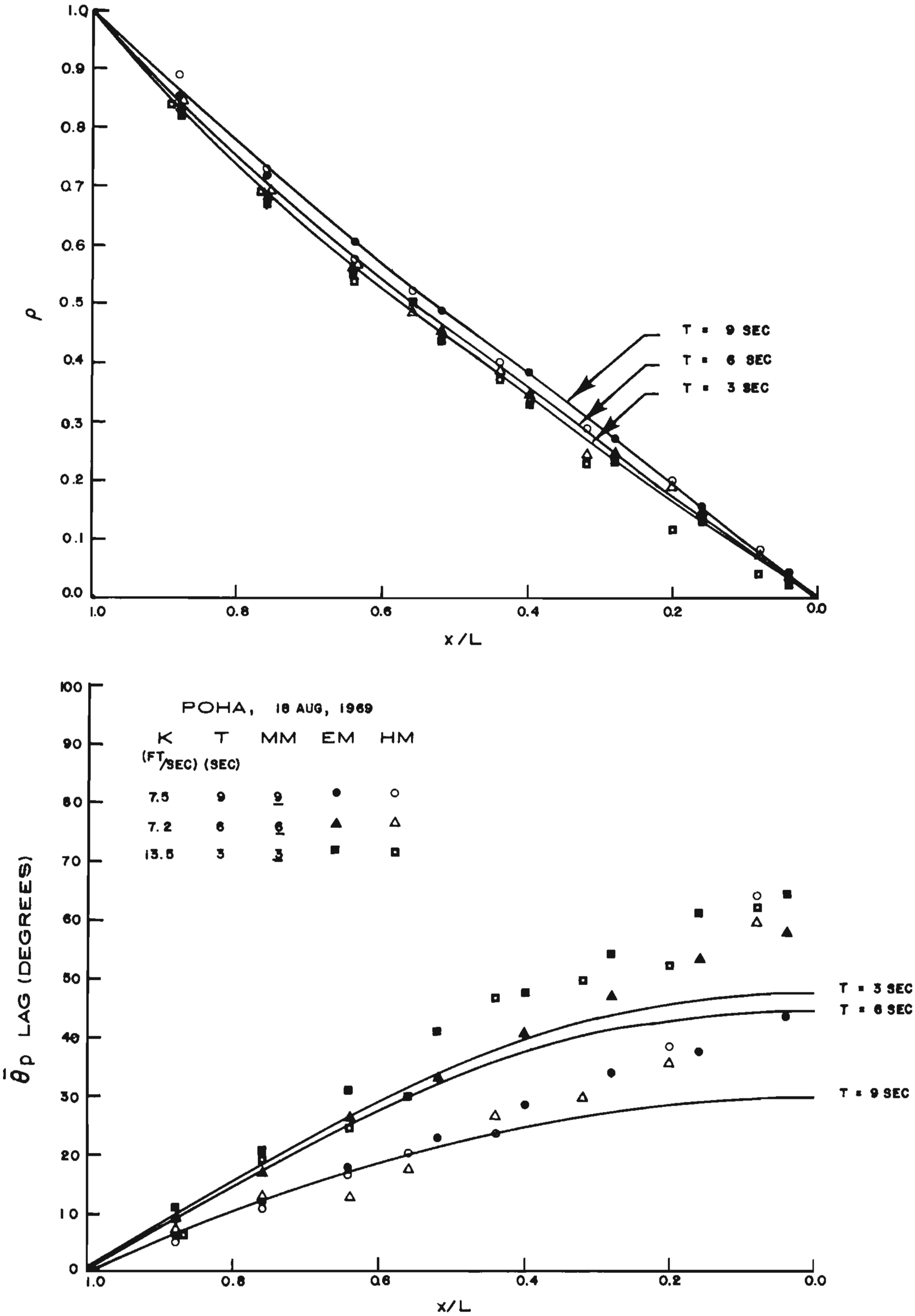

FIGURE 14. AMPLITUDE AND PHASE ANGLE VS x/L
FOR POHA, 18 AUG. 1969 DATA.

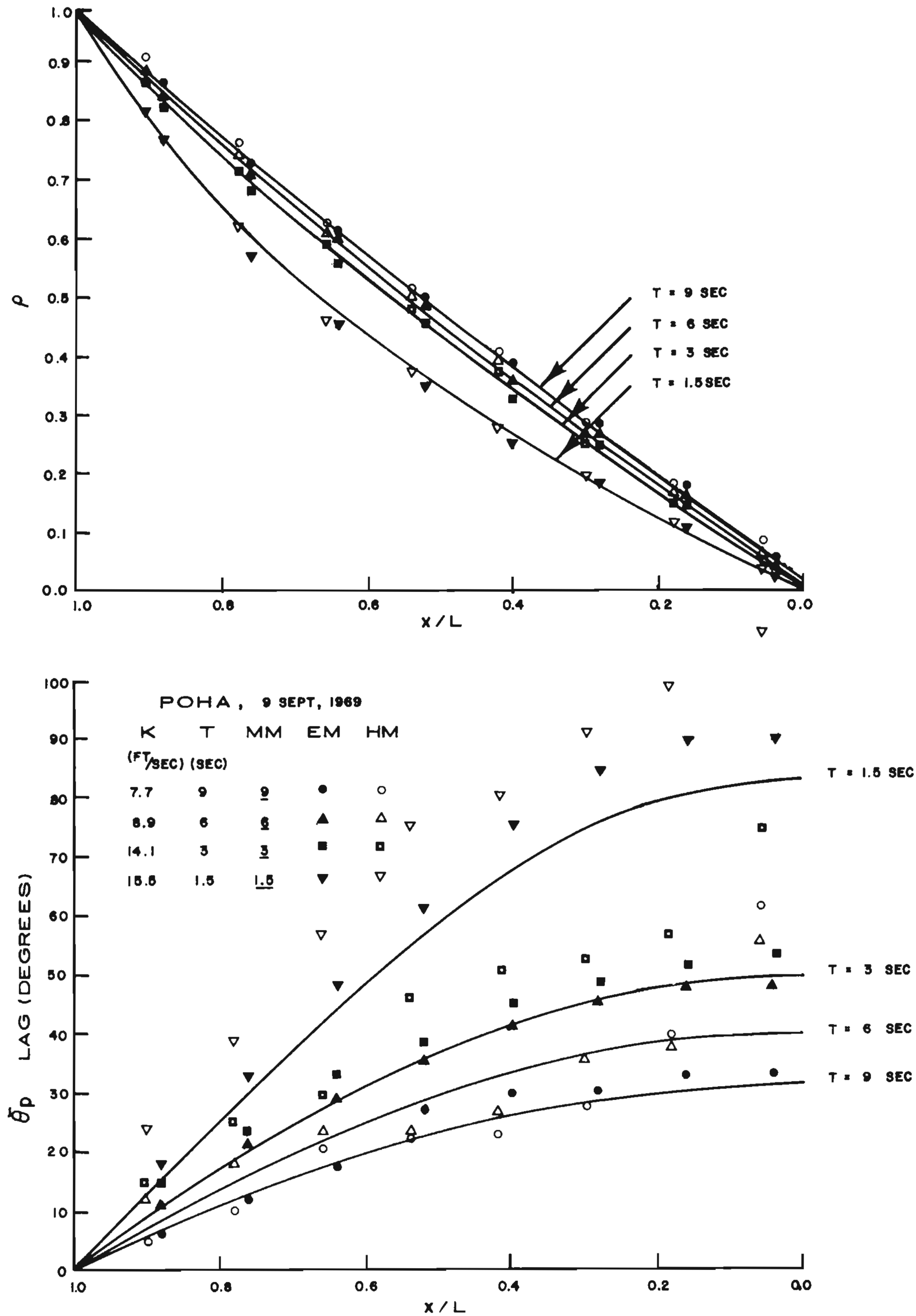

FIGURE 15. AMPLITUDE AND PHASE ANGLE VS x/L FOR POHA, 9 SEPT. 1969 DATA.

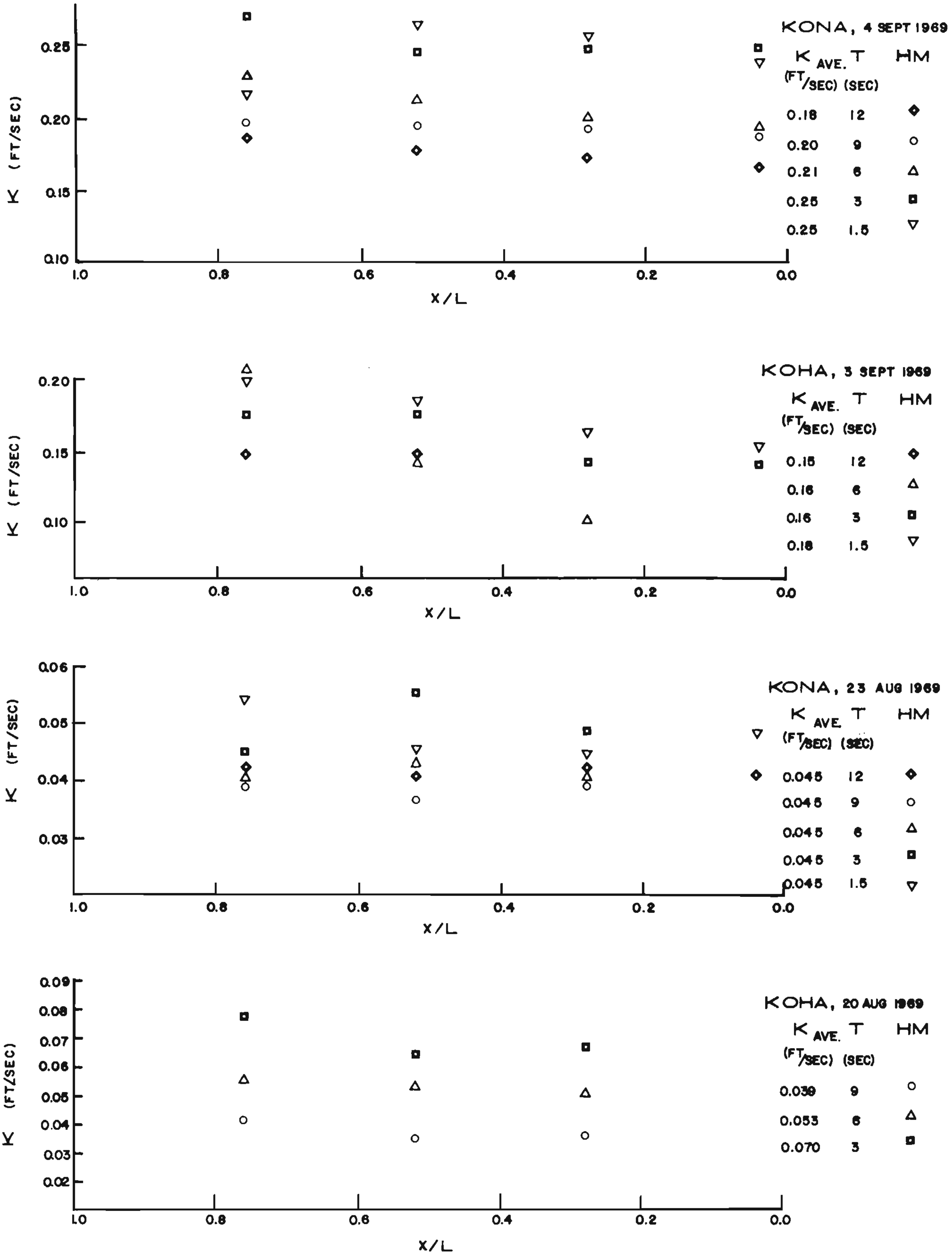

FIGURE 16. DARCY K VS x/L FOR KONA AND KOHA.

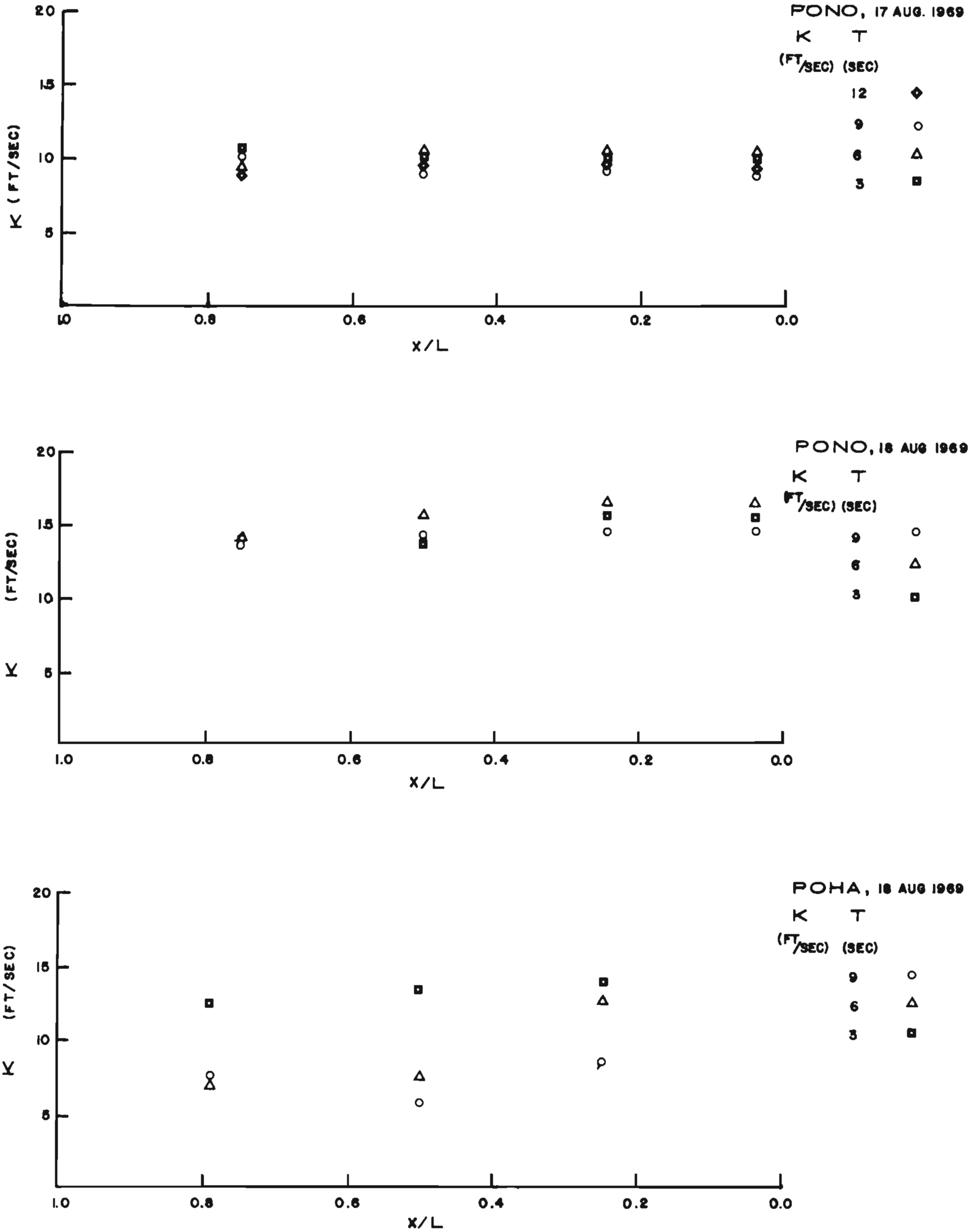

FIGURE 17. DARCY K VS x/L FOR PONO AND POHA, 17, 18 AUG. 1969 DATA.

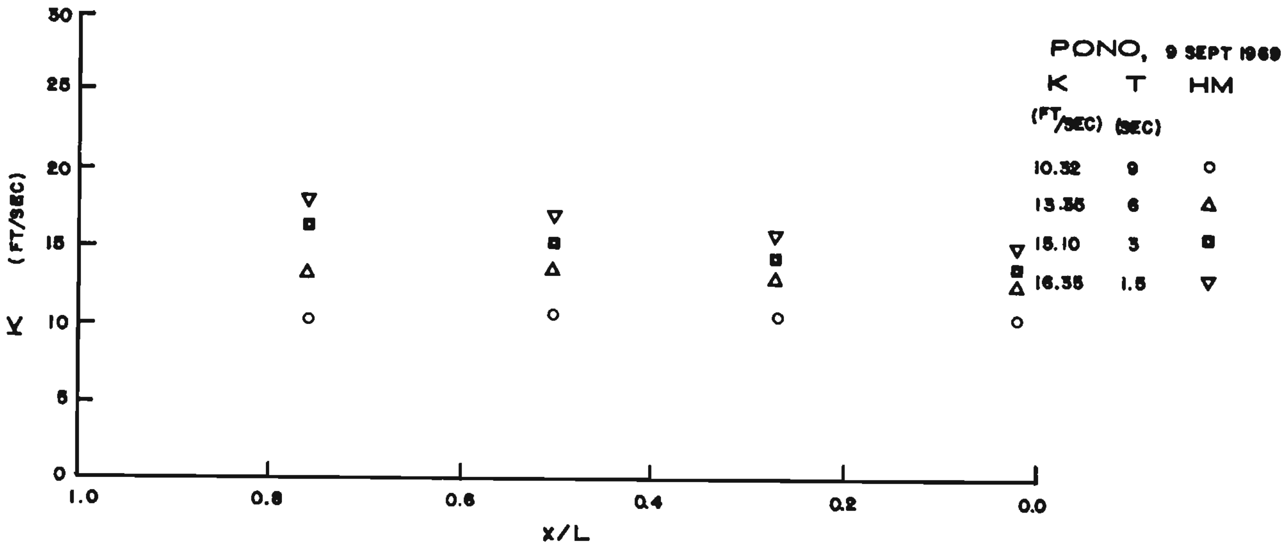

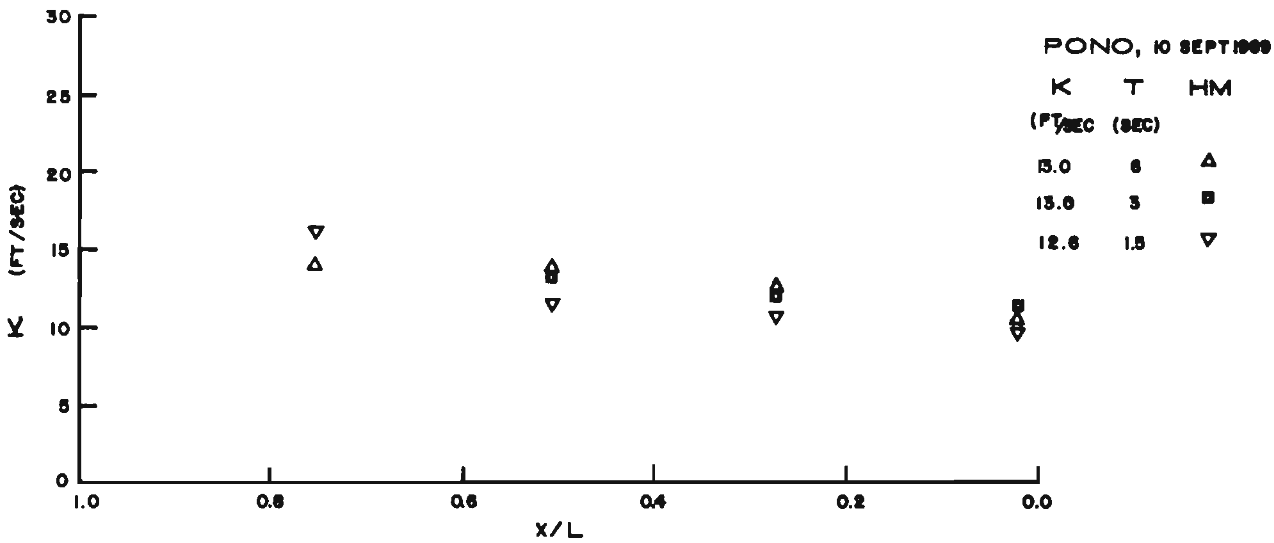

FIGURE 18. DARCY K VS x/L FOR PONO,
9, 10 SEPT. 1969 DATA.

proaches a linear variation in x. This is only possible if α tends to zero which requires that K become large. Hence, a slight amount of data scatter in the hydraulic model results produced large variations in K and the iteration process employed in the Newton-Rhapson method did not always converge to the correct value. For this reason the electric analog model was used as a computer to estimate K values. The procedure involved adjusting the audio-oscillator frequency until the amplitude and phase angles in the electric analog matched the hydraulic model data. This frequency was used to calculate K_4 and equations (12), (15), and (16) were then solved for K. The values of K recorded in Table 2 for the tests on POHA of 17 August and 9 September were determined in this way.

The Electric Analog Model Data

The analysis of the electric analog data was essentially the same as that used for the hydraulic model data. Amplitudes and phase angles were scaled off photographs similar to the one shown in Figure 4B. Amplitudes were normalized with respect to the amplitude of the input voltage by dividing the crest-to-trough distance of each trace by the crest-to-trough distance of the input trace. The phase angles were calculated by dividing the distance from the peak of the input trace to the peak of the trace in question by the distance between the two peaks of the input trace and multiplying the quotient by 360. In the photo, each major division on the vertical scale represents 0.1 volts. Each major division on the horizontal scale represents 60°. Since these major divisions are 1.0 cm apart on the face of the cathode ray tube, the scale factor for measuring phase angles is about 6°/mm.

The results from the electric analog model tests are presented in Figures 5 through 15 as plots of the normalized amplitudes and the phase angles as functions of the normalized distance from the coastline, x/L. These results are represented by the shaded symbols.

The Mathematical Model Results

The results from the mathematical model are also presented as plots of dimensionless amplitude and phase angles versus the dimensionless position, x/L. The ρ and Θ_p were computed from the equations given in "The Mathematical Model" section (p. 2) with the aid of the IBM 360 computer. Each average value of K (see Table 2) was incorporated into the calculations by adding an IBM card. The computer output gave ρ and Θ_p at ten evenly-spaced intervals along the media. The computer programs for ρ and Θ_p were identified as follows:

Konfined,[1] one-dimensional, no-flow boundary condition aquifer - KONA

Konfined,[1] one-dimensional, constant-head boundary condition aquifer - KOHA

Phreatic, one-dimensional, constant-head boundary condition aquifer - POHA

Phreatic aquifer, one-dimensional, no-flow boundary condition - PONO

Phreatic, one-dimensional cylindrical island aquifer - POCI

The mathematical model results are presented in Figures 5 through 15 and 19 and are represented by the solid curves. KONA and PONO are essentially the same program since the mathematical models for these two cases differ only in the expression for α. Likewise, KOHA and POHA are the same program, and POCI would also be applicable to the cylindrical island aquifer of constant thickness in the confined condition. The programs for KONA, KOHA, and POCI are written out in Appendix D. A sample of the computer output for the tests on 3 and 4 September 1969 is included.

Analysis of Miller's Data

Miller (1941) presented his basic data in the form of graphs similar to those in Figures 5 through 15. Since the conditions of his experiments were essentially identical to those for the hydraulic model tests described here, his data was analyzed as described above. That is, the Darcy permeability as a function of x was determined from the data, an average value of the permeability was then calculated, and finally, the average K was inserted into the computer program PONO and the theoretical amplitude and phase angles as functions of position were computed. The results are presented in Table 3 and Figure 20. Table 4 presents a comparison of the average value of the true permeability of the material, i.e., $k = (\mu/w_0)K = 2.35 \times 10^{-5}/62.4$ K, as calculated by Miller, with average values determined by the technique

---

1) *Konfined* is used for confined.

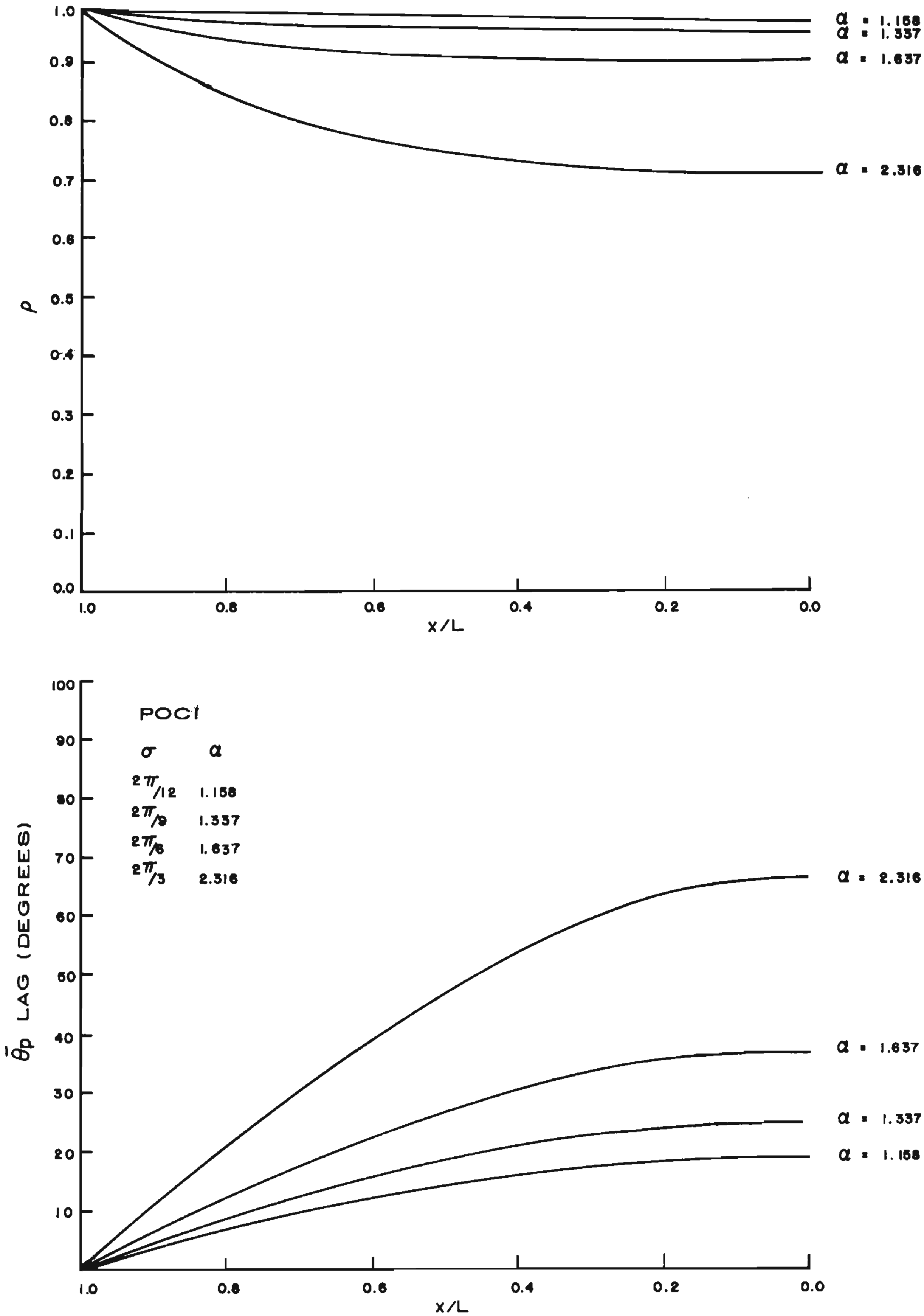

FIGURE 19. AMPLITUDE AND PHASE ANGLE VS x/L FOR POCI.

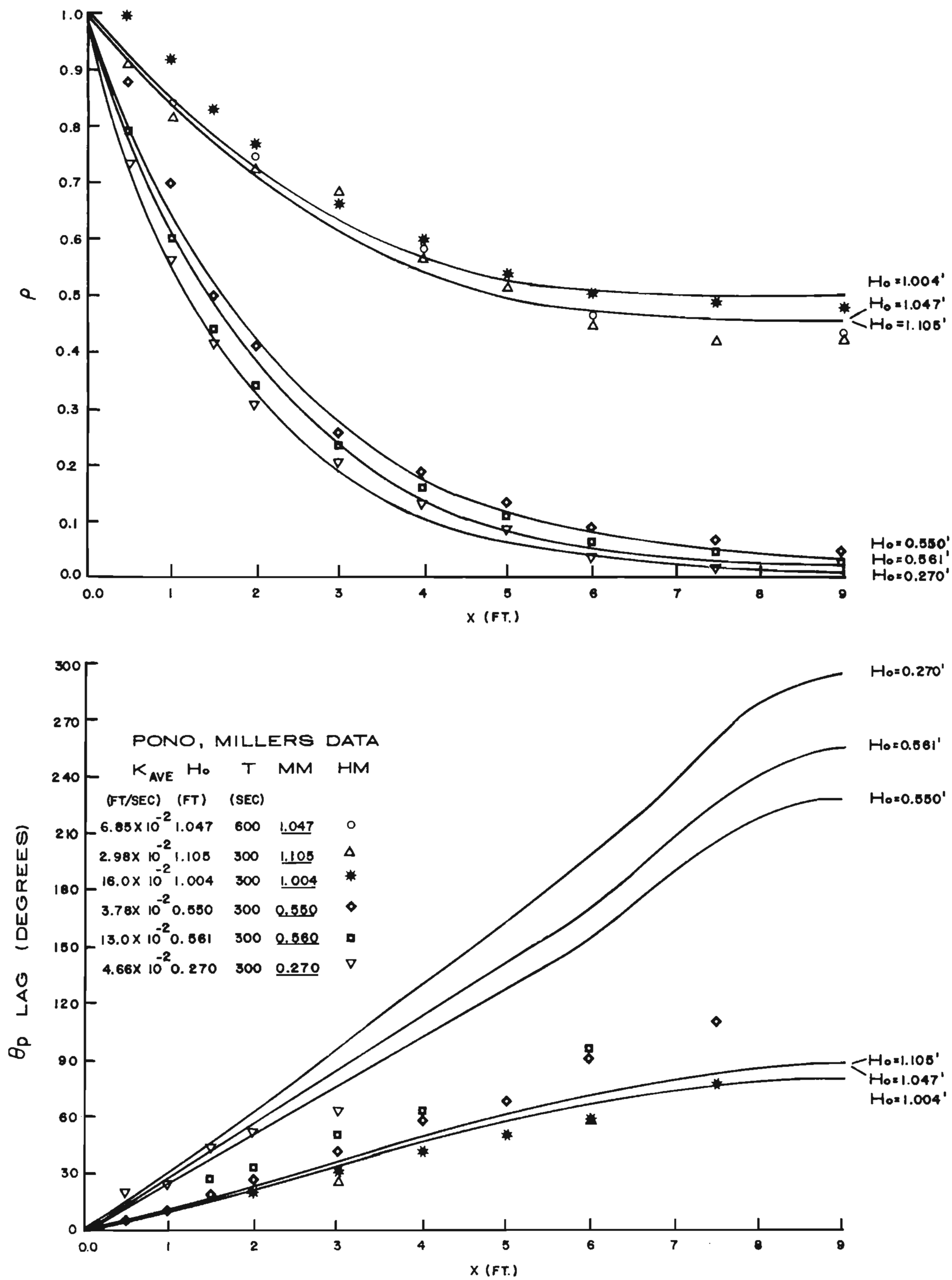

FIGURE 20. AMPLITUDE AND PHASE ANGLE VS x FOR MILLER'S DATA.

TABLE 3. SUMMARY OF MILLER'S DATA.

H_0[1] FT.	h_0[2] FT.	T[3] SEC.	DIMENSIONLESS AMPLITUDE/DARCY PERMEABILITY IN FT./SEC. AT THE INDICATED POSITION, x/L			
			.750 = x/L	.500 = x/L	.250 = x/L	.062 = x/L
1.047	0.10	600	0.690 7.52×10^{-2}	0.525 7.23×10^{-2}	0.435 6.24×10^{-2}	0.430 6.36×10^{-2}
1.105	0.10	300	0.690 2.35×10^{-2}	0.525 3.17×10^{-2}	0.430 3.34×10^{-2}	0.430 3.05×10^{-2}
1.004	0.05	300	0.725 18.5×10^{-2}	0.535 15.5×10^{-2}	0.475 14.8×10^{-2}	0.470 14.8×10^{-2}
0.550	0.05	300	0.340 3.23×10^{-2}	0.125 3.52×10^{-2}	0.060 4.40×10^{-2}	0.040 3.95×10^{-2}
0.561	0.10	300	0.285 14.2×10^{-2}	0.115 13.7×10^{-2}	0.040 11.95×10^{-2}	0.025 12.05×10^{-2}
0.270	0.05	300	0.250 4.02×10^{-2}	0.080 4.82×10^{-2}	0.020 4.67×10^{-2}	0.015 5.14×10^{-2}

[1] H_0 = AVERAGE WATER DEPTH IN AQUIFER.
[2] h_0 = AMPLITUDE OF THE FLUCTUATION IN PIEZOMETRIC HEAD AT THE "COASTLINE."
[3] T = PERIOD OF SINUSOIDAL FLUCTUATIONS IN PIEZOMETRIC HEAD.

TABLE 4. COMPARISON OF COEFFICIENTS OF PERMEABILITY FOR MILLER'S DATA.

CONDITIONS			AVG. COEFFICIENT OF PERMEABILITY $K \times 10^{10}$ FT.^{2}	
H_0, FT.[1]	h_0, FT.	T, SEC.	L = INFINITY	L = 9.6 FT.
1.047	0.10	600	378	258
1.105	0.10	300	697	112
1.004	0.05	300	770	598
0.550	0.05	300	142	142
0.561	0.10	300	115	488
0.271	0.05	300	152	175

[1] REFER TO TABLE 1 FOR AN EXPLANATION OF THE TABLE HEADINGS.

described above. The basic difference is that Miller's calculation assumes an aquifer of infinite length, and the method used here is based on equations (4a), (4b), and (4c), which account for the finite length of the model. That is, if $L = \infty$, then in equation (2c) C_1 must be zero and the solution takes the form

$$\zeta(x,t) = \zeta_0 e^{-\sqrt{\frac{\alpha}{2}}x} \sin\left(\sqrt{\frac{\alpha}{2}}x - \sigma t\right) \tag{17}$$

where the aquifer extends over the region $x \geq 0$.

Miller also ran permeability tests on the sand. Variable-head permeability tests gave the permeability as 5.35×10^{-10} square feet, and tests made with sand in place in the channel under steady-state conditions gave 9.5×10^{-10} square feet. The latter is an average of values of K computed from the slope of the free surface at several points along the test section.

DISCUSSION OF RESULTS

The Coefficient, α

The analysis of the hydraulic model data has assumed, for purposes of calculation, that the changes in the coefficient, α, resulting from changes in the experimental conditions such as aquifer thickness, tidal period, etc., can be expressed as variations in the Darcy coefficient of permeability (see Figs. 16, 17, and 18). However, in a given fluid, K depends only on a characteristic length of the porous structure of the media and hence should not change appreciably under the experimental conditions used in this study. Therefore, the other factors in the coefficient, α, are more likely to assume the major part of any changes. For the confined aquifer it is the specific storage that will probably vary, and for the polyurethene foam, this amounts to a change in the Young's modulus as $1/E \gg \varepsilon/\beta$. For the unconfined aquifer the porosity is the more likely to undergo a major change.

The Confined Aquifer Models

Figure 16 reveals a dependence of permeability on the aquifer thickness, on the tidal period, on the position within the aquifer at which it is evaluated, and on the boundary condition at $x = 0$.

The permeability for the aquifer composed of two layers of foam ($b = 5.875$ inches) is about three times larger than that for the aquifer composed of one layer of foam ($b = 2.875$ inches). This difference is largely the result of a change in the Young's modulus rather than a true change in the permeability. The polyurethene foam did not deform uniformly over its depth. The material in the immediate neighborhood of the applied load underwent the maximum deformation and, therefore, exhibited the greatest compressibility and, hence, the largest specific storage. Thus, the confined aquifer models with two layers of foam had a smaller average specific storage, over its depth, than that for the models with just one layer of foam. Furthermore, the good agreement between the K values, determined from the permeability tests, and those calculated from the two-layer foam model indicates that this non-uniform compressibility is confined to a region small enough to permit the foam to behave essentially in the same way as it did in the permeability tests.

An additional factor affecting the compression of the foam was the non-uniformity of the aquifer cross section. The plastic bag of water which confined the aquifer adhered to the sides of the tank, causing the aquifer to compress more in the central region than at the edges. This difference in thickness amounted to about 0.25 inches for both the one- and two-layer aquifers. For this reason, an average thickness of 2.875 inches or 5.875 inches was used in the calculation of K. The fact that the upper confining surface of the aquifer offered more resistance to vertical motion at the edges than at the center resulted in a non-uniform deflection of the media, contrary to one of the assumptions upon which equation (1a) is based. This effect of the non-uniformity has relatively less influence as the thickness of the aquifer increases.

Figure 16 indicates that the lower frequency tidal changes yield the smaller coefficients of permeability. Again, it would seem more likely that a change in the specific storage takes place with a tidal period, rather than a true variation of K, provided the flow remains laminar. That is, as the tidal frequency increases the specific storage must decrease and, hence, Young's modulus would increase and require a smaller vertical deflection of the media for a given change in the vertical load. This is consistent with the physical behavior of the foam since the magnitude of the deflection depends on the time the load is applied.

There is a general tendency for the permeability to increase slightly with distance from the internal boundary, although for the tests on KONA on 23 August 1969, K remains essentially constant for the 12, 9, and 6-second period tide and exhibits a slight decrease with distance from the internal boundary for the 3-second period tide. This tendency is probably the result of a secondary flow of water under the bulkhead that partitioned off the tidal compartment and into the volume bounded by the foam, the plastic bag, the bulkhead, and the tank walls (i.e., into the corners where the bag was not completely seated). The larger pressures that developed near the coastline as a result of the secondary flow render values of K calculated from amplitudes scaled off the pressure records correspondingly too large.

The variations of K with the boundary conditions exhibit no pattern and are most likely the result of experimental error. That is, the end compartments in the hydraulic model were only 48.0 square inches in cross-sectional area; hence, changes in the water surface elevation at $x = 0$ were observed for the longer periods tested. These observed variations in the head are recorded in the last column of Table 1. For the 12-and 9-second tidal periods, these variations are substantial and influence the response of the aquifer over a region larger than just the immediate vicinity of $x = 0$.

Based on an average K selected from Figure 16, the results of the mathematical and electric analog models compare very favorably with the hydraulic model data given in Figures 5 through 8. The electric analog model results are independent of the scale factor, K_2, as can be seen by eliminating K_2 between equations (15) and (16) and substituting the results into equation (12). The electric circuit is not subject to the same restrictions that are imposed on the physical model, i.e., small amplitude fluctuations with respect to water depth, etc.

The Unconfined Aquifer Model

Figures 17 and 18 indicate that the Darcy permeability depends, essentially, on the same quantities as the confined aquifer model. In particular, it appears to depend upon the average water depth, the tidal amplitude, the tidal period, the location, and the boundary condition at $x = 0$. It is more reasonable to assume that, for the unconfined model, it is the porosity rather than the permeability that changes. An apparent porosity can be easily calculated from the expression

$\varepsilon' = \varepsilon(K/K')$, where $K = 0.20$ ft./sec and is considered to be representative of the permeabilities determined from the permeameter tests (see Appendix B), K' is one of the average values of the coefficient of permeability recorded in Table 2, and $\varepsilon = 0.97$, the true porosity of the foam. The same calculations can be made for Miller's data using $k = 5.35 \times 10^{-10}$ ft.^{2} and the average values of the permeability for the finite aquifer presented in Table 4.

As a result of surface tension a partially saturated region forms above the equilibrium level in the media where the porosity varies from zero at the equilibrium plane to its true value, ε, at the upper edge of the region. For polyurethene foam this region is about one inch thick. Consequently, the thickness of this zone relative to the tidal amplitude and the average water depth becomes important in determining the response of the aquifer to the tidal change of a given period. A dimensionless combination of these three variables is $\sqrt{g\bar{z}}/\zeta_0 T^{-1}$. This quantity can be interpreted as the ratio of the velocity of a long wave in shallow water to one-fourth the average velocity of the vertical displacement of the free surface at a given point as the long wave passes by. It can also be considered as the ratio of the length of a long wave of period T to its amplitude. The effect of tidal period, tidal amplitude, and average water depth on the porosity can be studied by plotting ε'/ε versus this dimensionless variable. This plot is presented in Figure 21 and reveals the following facts:

1. As the amplitude of the tide increases, the apparent porosity increases for both PONO and POHA. (See Table 1 and compare the test results of 17 August with the other test results.)
2. As the period of the tide increases, the apparent porosity increases quite sharply for POHA, but remains essentially constant for PONO.
3. A comparison of Miller's data with the data from PONO indicates that the porosity ratio for the foam is of the same order of magnitude as that for the sand.

The first fact can be explained by noting that the larger tidal amplitudes produce larger vertical displacements of the piezometric

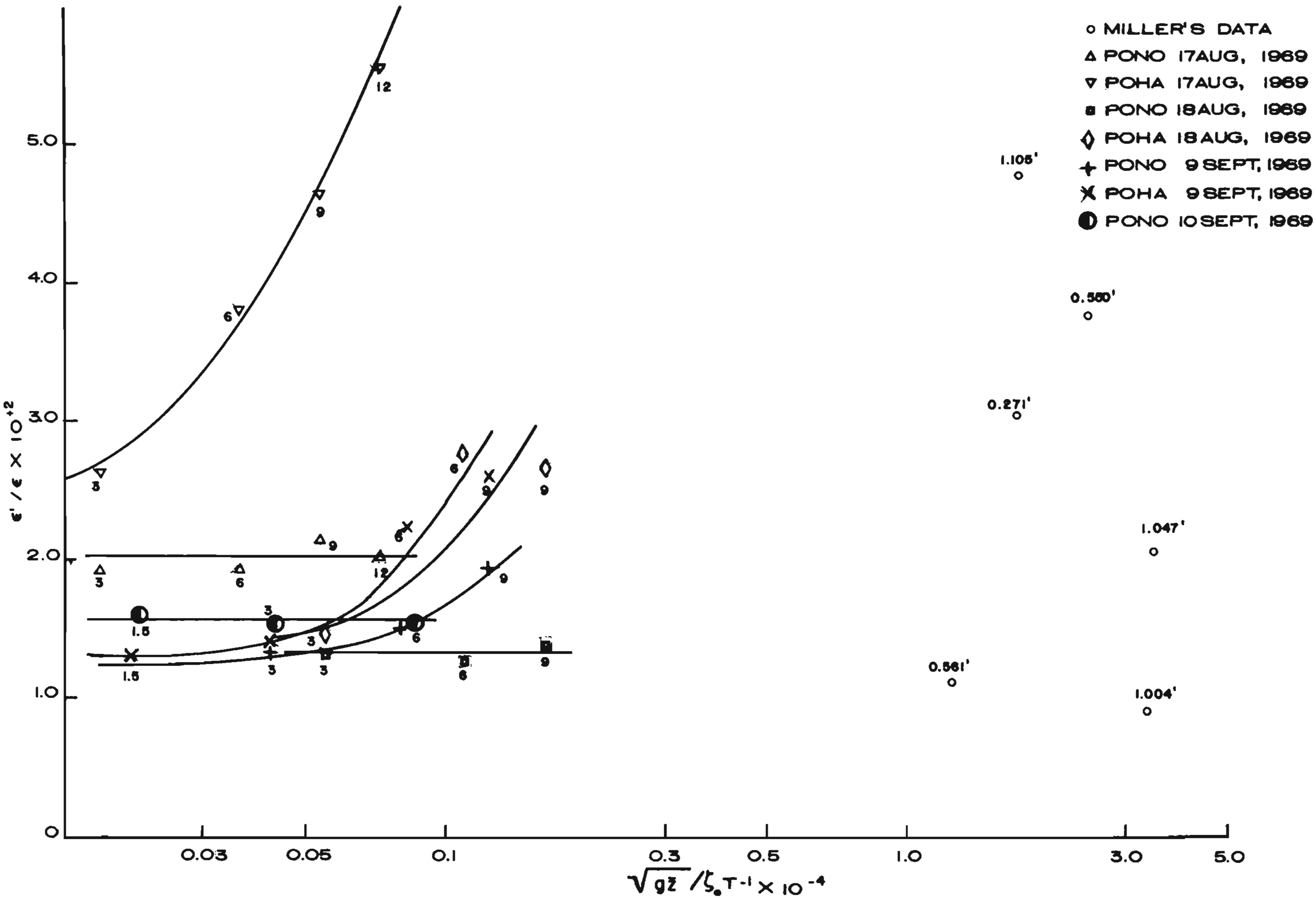

FIGURE 21. VELOCITY RATIO, $\sqrt{g\bar{z}}/\zeta_0 T^{-1}$ VS POROSITY RATIO, ε'/ε.

surface, causing it to rise further into the less saturated portion of the capillary fringe zone. Thus, the water moves into a region which has on the average an increasingly greater porosity. This apparent porosity should approach the true porosity as the tidal change becomes large with respect to the thickness of the capillary fringe zone. It should be noted that the tests on 17 August involved a water depth about twice as large as that used for the remainder of the tests. However, it is unlikely that this difference in the average water depth had any significant influence on the increase in porosity ratio as the tidal amplitude was adjusted to keep the ratio $\zeta_o/\bar{z}$ small.

The second fact is the result of not having the constant-head boundary condition at $x = 0$ strictly satisfied. The change in head at $x = 0$ lagged only slightly behind the change at $x = L$ and, therefore, less water moved through the aquifer during a tidal cycle, resulting in an increased displacement in the tidal compartment of the model. These greater tidal changes produced larger phase lags and an increased rate of decay of the amplitude of the head-change with distance from the coast. The increased decay rate occurred over approximately sixty percent of the aquifer length. Hence, the dimensionless amplitudes calculated from hydraulic model data taken on the range of $0.4 \leq x/L \leq 1.0$ were smaller than if the constant-head boundary condition had been satisfied. These small values of ρ result in smaller values of the calculated Darcy permeability or in larger values of the apparent porosity. It is worth noting that the porosity curves for PONO and POHA converge as the period decreases and the constant-head condition is more nearly satisfied. The increase in porosity with period for PONO of 9 September 1969 is probably the result of leakage under a poorly-sealed bulkhead at $x = 0$.

Miller's data in Figure 21 exhibits a considerable amount of scatter and no trend,with respect to the several variables involved, is present. Since the thickness of the capillary fringe zone in the Sacramento River sand was surely greater than 0.1 feet, a comparison with the present tests should probably exclude the data for PONO, 7 August 1969, where the tidal amplitude was equal to the thickness of the capillary fringe zone. All of the data from the present tests, however, falls within the range of scatter of Miller's data.

Figures 9 through 15 indicate that the mathematical model and the electric analog model give good agreement with the hydraulic model if the apparent porosity (or the apparent permeability) is used.

The Applicability of Darcy's Law

In steady flows the applicability of Darcy's Law requires that the Reynolds number based on a representative grain size be less than 10. An estimate of the Reynolds number can be made using the head changes at $x = 0$, as recorded in Table 1. The largest average velocity was developed for a tidal period of 12 seconds using the unconfined hydraulic model. A vertical change of 0.25 inches in the 6-inch x 8-inch end compartment over a 6-second interval implies an average velocity through the 6-inch x 10.375-inch cross section of foam of about 3×10^{-3} ft./sec. For a kinematic viscosity of 1.0×10^{-5} ft./sec. and a representative "grain size" of 3×10^{-4} ft. (0.1 mm) the Reynolds number is approximately 0.1. Reynolds numbers, which are somewhat larger, may develop locally. For example, the steepest gradients in the piezometric head develop at the coastline, $x = L$, where the vertical motion is the largest and when the piezometric surface is in its equilibrium position. Darcy's Law can be used to estimate a velocity. The gradient in the piezometric head at $x = L$ (where $\rho = 1$ and $\Theta_p = 0$) from equations (4) or (5) is $\partial\zeta/\partial x = \zeta_o \, \partial\Theta_p/\partial x$. From Figure 5, the maximum rate of change in phase angle is of the order $\pi/2$ radians/foot. Thus, the maximum Reynolds number in the vicinity of the coastline is approximately 5K, or 1.0, for $K = 0.20$ ft./sec. Thus, the Reynolds number criteria appears to be satisfied.

The Cylindrical Island Aquifer

The results obtained from the mathematical model for an island aquifer represent a cylindrical island with a radius of 4.0 feet and a Darcy permeability of 0.2 ft./sec. If a confined aquifer is to be considered, the curves correspond to an aquifer whose specific storage is 0.032 $(\text{feet})^{-1}$; if an unconfined aquifer is considered, the curves correspond to an aquifer whose effective porosity is about 1.5×10^{-2}

and whose average water depth is 0.5 feet. A comparison with the results from KONA on 4 September 1969 shows the effect of convergence in a radial flow. Both the damping of the oscillations and their phase difference with respect to the tide have been reduced.

CONCLUSIONS

The results of these tests can be summarized in the following conclusions:

1. Diffusion theory can be applied to analyze the response of aquifers to tidal changes provided the boundary conditions are known and the assumptions implicit in the theory are not seriously violated.[1] A direct consequence of the validity of the diffusion theory is the applicability of the electric analog model.
2. In studying confined aquifers, it will be necessary to use an apparent specific storage coefficient if the compressibility of the aquifer skeleton is modified by bridging or arching or other structural anomalies.
3. In studying unconfined aquifers, it will be necessary to deal with an apparent porosity because of the presence of the capillary fringe zone. This apparent porosity should approach true porosity as the tidal amplitude becomes large compared with the thickness of the capillary fringe zone. Also, the wave length in the media should be large compared with the average aquifer depth to assure the satisfaction of the Dupuit assumptions.
4. A comparison of the porosity ratios (ε'/ε) for the tests described here and for Miller's tests on the Sacramento River sand shows that the two are of the same order of magnitude and that the apparent porosity varies over the range, $1.0 \times 10^{-2}\,\varepsilon \leq \varepsilon' \leq 5.0 \times 10^{-2}\,\varepsilon$, with an average value of about 1.5×10^{-2}. Further research is required to delineate more precisely the relationship between apparent porosity and tidal amplitude.

[1] In order to minimize the effect of local coastal geometry, observations should be made at a distance of 8 to 10 average aquifer thicknesses from the coastline.

ACKNOWLEDGEMENTS

The authors would like to express their appreciation to Mr. Griffith Woodruff, director of the machine shop at the Center of Engineering Research, University of Hawaii, for his assistance in the design and construction of the hydraulic model tank and the tidal generator. We would also like to thank Mr. Garrett Okada, Junior in Civil Engineering, for this help in the construction of the hydraulic model and Mr. T. D. Krishna Kartha, Assistant in Hydrology, for his help in constructing and testing the initial electric analog models. Finally, we would like to thank Mrs. Rose Pfund and her publication staff for their help in publishing this report.

REFERENCES

Bear, J., D. Zaslavsky, and S. Irmay. 1968. *Physical principles of water percolation and seepage.* United Nations Educational, Scientific and Cultural Organization, Paris.

Carr, P. A. and G. S. VanderKamp. 1969. "Determination of aquifer characteristics by the tidal method." *Water Resources Research,* V, v, pp. 1023-1031.

De Weist, R. J. M. 1965. *Geohydrology.* John Wiley & Sons, Inc., New York.

Jacob, C. E. 1950. "Flow of ground water." *Engineering Hydraulics,* edited by Hunter Rouse, John Wiley & Sons, Inc., New York.

Karplus, W. J. 1958. *Analog simulation.* McGraw-Hill Book Company, Inc., New York.

McCraken, D. A. 1967. *Fortran IV manual.* John Wiley & Sons, Inc., New York, 4th printing.

McLachlan, N. W. 1934. *Bessel functions for engineers.* Oxford University Press, London.

Miller, R. C. 1941. "Periodic fluctuation of homogeneous fluid with free surface in porous media." (Thesis, Master of Science in Civil Engineering, University of California.)

Prinz, E. 1923. *Hydrologie.* Verlag Springer, Berlin.

Sneddon, I. N. 1961. *Special functions of mathematical physics and chemistry.* Oliver and Boyd, Edinburgh and London.

System/360 scientific subroutine package. 1968. IBM Technical Publications Department, New York.

Todd, D. K. 1954. "Unsteady flow in porous media by means of a Hele-Shaw viscous fluid model." *Transactions,* American Geophysical Union, XXXV, vi.

Walton, W. C. and T. A. Prickett. 1963. "Hydrogeologic electric analog computers." *ASCE Journal of Hydraulic Division,* HY-6, pp. 67-91.

Werner, P. W. and D. Noren. 1951. "Progressive waves in non-artesian aquifers." *Transactions.* American Geophysical Union, XXXII, ii, pp. 238-294.

APPENDICES

APPENDIX A. LIST OF SYMBOLS AND ABBREVIATIONS

a	Characteristic length in hydraulic model
b	Thickness of porous media
C	Capacitance, farads
C_D	Diffusion coefficient
C_1, C_2, C_3	Complex constants
e	Base of natural logarithms
E	Young's Modulus, psi
h	Piezometric head, ft
i	$\sqrt{-1}$ and electric current, amps
J_0	Bessel Function of first kind, of order zero
k	Permeability, $(ft)^2$
K	Darcy coefficient of permeability, ft/sec
K_1, K_2, K_3, K_4	Scale factors for electric analog model (see Sec. III)
L	Length of porous media, radius of porous island
q	Volume $(ft)^3$
Q	Discharge $(ft)^3$/sec
$\mathcal{Q}$	Quantity of charge, coulombs
R	Resistance, ohms; the real part of
r	Space variable, radial direction
S	Coefficient of storage
S_s	Coefficient of specific storage $(ft)^{-1}$
t	Time variable
T	Coefficient of transmissability, $(ft)^2$/sec, tidal period, sec
V	Electric potential, volts
w_0	Specific weight of water, lbs/$(ft)^3$
x, y, z	Space variables
Y_0	Bessel Function of the second kind, of order zero
$\bar{z}$	Average water depth, ft
α	$S\sigma/T$ for confined aquifer model, $\varepsilon'\sigma/K\bar{z}$ for unconfined aquifer
β	Bulk modulus of water, psi
ε	Porosity
ε'	Apparent porosity

ζ	Piezometric surface referenced from the equilibrium plane
ζ_o	Amplitude of tidal change
η	That part of the piezometric surface which depends only on the space variable
θ_ρ	Phase angle, degrees
ρ	Dimensionless amplitude = ζ/ζ_o
σ	Angular frequency, rad/sec
KONA	Confined, one-dimensional, no-flow boundary condition aquifer
KOHA	Confined, one-dimensional, constant head boundary condition aquifer
POHA	Phreatic, one-dimensional, constant head boundary condition aquifer
PONO	Phreatic aquifer, one-dimensional, no flow boundary condition
POCI	Phreatic, one-dimensional cylindrical island aquifer

APPENDIX B

The Porosity, Compressibility and Permeability of Polyurethene Foam

POROSITY TEST. The porosity of the polyurethene foam was determined from the following equation:

$$\varepsilon = \frac{V_v}{V_t} = \frac{V_t - V_s}{V_t} = \frac{V_t - V_w}{V_t} \quad ,$$

where V_v = volume of voids
V_t = total volume of sample
V_s = volume of solids
V_w = volume of water displaced by sample.

First, the volume and weight of the sample were determined. A 1000-ml florence flask was filled with water to a given level, weighed and then emptied. Next, the polyurethene sample was cut into strips and inserted into the florence flask. The flask was filled with water and a glass rod was used to compress the foam strips to remove some of the entrapped air. Then the flask was connected to a vacuum pump to draw off the remaining trapped air. Water was added to the flask to bring the meniscus to the same level as before and the flask was weighed. The volume of water displaced was calculated by using the following equations:

$$W_1 - W_2 = W_w \quad ,$$

$$V_v = \frac{W_w}{\gamma_w}$$

where W_1 = weight of beaker + water + dry sample
W_2 = weight of beaker + water + submerged sample
W_w = weight of water displaced
γ_w = unit weight of water.

The porosity of the foam was then calculated using the values of V_t and V_v as determined by the above procedure.

A second method used in finding the volume of displaced water was to immerse a foam sample in a clear lucite cylinder filled with water. The sample was kneaded and squeezed to eliminate as much of the trapped air as possible, and the new water level was noted. The volume of displaced water was calculated from the following equation:

$$V_w = \Delta h(A)$$

where Δh = difference in water levels

A = cross sectional area of lucite cylinder

The porosity was then calculated as in the previous test.

The calculated porosity resulting from the first method was 0.97 while that resulting from the second method was 0.96.

COMPRESSIBILITY TEST. The compressibility of a foam sample was determined from the slope of its stress-strain curve.

A cylindrical section of foam 5 inches in diameter and 2-15/16 inches high was cut to fit snugly into a cylindrical PVC container with approximately the same diameter. After the sample was placed in the container, a circular metal plate with a diameter slightly less than the inside diameter of the container was placed on top of the foam sample.

The PVC container was placed on the base plate of a Bridgeport vertical milling machine and a Soil Test proving ring placed on top of the metal plate on the foam sample. The base of the milling machine was moved vertically by using a control handle which was calibrated to show the vertical movement of the base to the nearest thousandth of an inch. The base was raised until the proving ring made contact with the top bearing area of the milling machine and the zero was set on the control handle scale. The base of the machine was raised further until the dial gage on the proving ring registered a deflection corresponding to a 1-lb load as determined from the calibration curve for the proving ring. The deflection of the foam sample was then read from the control handle scale. The load was increased by 1/2-lb increments up to 5-lb and the deflection noted for each load. Deflections of the proving ring were subtracted from the total deflection to obtain the deflection of the foam.

The stress-strain curve is plotted in Figure B1-1, and the

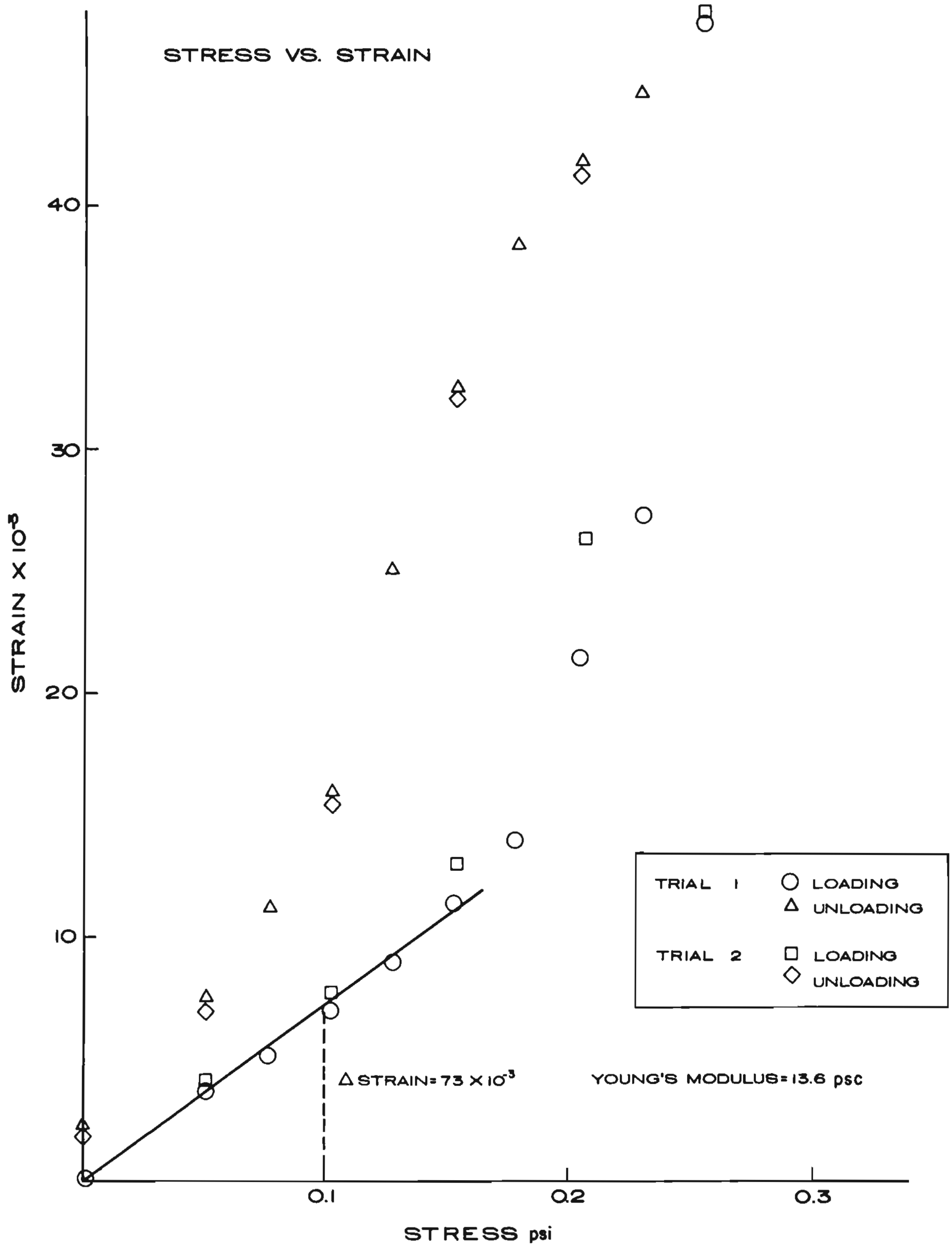

FIGURE B1-1. THE STRESS-STRAIN CURVE.

resulting Young's modulus of the foam is 13.6 psi.

PERMEABILITY TESTS. Permeability tests were conducted using both a small vertical cylindrical permeameter and the hydraulic model itself with the polyurethene foam in place.

Permeameter Tests. The specimens were cut with diameters approximately 0.125 inches larger than the permeameter to insure a snug fit.

The permeameter was connected with rubber tubing to a constant-head tank which was continuously supplied with water. The permeameter and the polyurethene samples were submerged and the samples squeezed to remove the trapped air. Then the samples were placed in the permeameter and both were taken out of the water.

The tests were run by noting the head loss over a given length of sample and the volume of water collected over a given period of time. Calculation of the permeability was based on the equation:

$$K = \frac{(V/t)L}{Ah} ,$$

where A = cross-sectional area of the sample

L = length

h = head loss over length, L

V = volume of water collected in time, t.

Different rates of discharge were obtained by changing the elevation of the permeameter with respect to the constant-head supply.

Since a small diameter plastic piezometer tube was used to determine the head at the lower end of the sample, a correction for capillary rise was subtracted from the head measurement. This correction factor was obtained by filling the permeameter with water and observing the difference between the height of the water in the tube and the height of water in the permeameter.

The polyurethene samples were taken from a larger sheet of foam and were cut in such a way that their axes of symmetry coincided with either the length, y, the width, x, or the depth, z, of the sheet.

Hydraulic Model Tests. The tubing from the tidal chamber pressure tap to the pressure transducer was disconnected at the transducer end and used as a discharge outlet into a collecting tank.

A rubber hose with a gate valve attached to one end supplied the inflow. The gate valve end was immersed in a bucket which was continuously supplied with water to give a constant-head supply. The opposite end of the hose was placed in the upstream compartment of the model tank. The gate valve was adjusted until a steady-state water surface profile was achieved. (This condition produced a straight line on the recorder chart.)

The pressure at several different pressure taps was recorded on the chart. The differences in pressure (number of lines) were converted into feet of water by using a calibration constant, 1 mm = .020 feet. The relative elevations of the pressure taps were determined by using a Wild tilting level. The difference in the elevations between two pressure taps, Δh, was added to the difference in pressure heads, Δy, to obtain the total head difference, ΔH, between the two points. (The distances, Δh, were about one or two millimeters and, therefore, of the same order of magnitude as Δy.) An average water surface slope was obtained by dividing the difference in water surface elevation, ΔH, between two pressure taps by the distance between the taps, Δx.

The discharge was determined by recording the volume of water collected from the outlet in a graduated cylinder over a fixed period of time.

K was determined by using the Dupuit equation:

$$K = \frac{V/t}{b\bar{y}\ \Delta H/\Delta x} ,$$

where V = volume of liquid collected in time, t

b = width of sample

ΔH = head drop in distance, Δx

$\bar{y}$ = average water surface elevation over the length, Δx.

The same hydraulic model set-up as in the previous test was used, but a Wild tilting level and point gage were used to determine the head difference between the two ends of the foam.

A point gage with a ruler graduated in millimeters fastened to it was placed in the upstream compartment.

A Wild tilting level was set up along side the hydraulic model and a line of sight established. After a steady state condition was established by adjusting the gate valve, the pointer was moved until it just touched the water surface, and the point where the line of sight intersected the ruler was noted. The point gage was then moved to the downstream compartment and adjusted until the line of sight of the level again intersected the ruler at the point previously noted. The dial indicator on the point gage was reset to zero, and the pointer moved until it touched the water surface. The deflection shown on the dial indicator was equal to the head loss across the hydraulic model.

The discharge was determined as described above.

The Darcy permeability was again calculated from the Dupuit equation with $\Delta x = L$, the length of the foam.

A steady-state flow condition was difficult to maintain, hence, the moving and adjusting of the point gage had to be carried out quickly.

FALLING HEAD PERMEABILITY TEST. The hydraulic model of a confined aquifer was also used as a falling-head permeameter. The discharge outlet used for the unconfined model tests was sealed off.

The water depth in both the upstream and the downstream compartments was set initially at 9 or 10 inches. Using a bucket of water, the upstream compartment was quickly filled to approximately 13 to 14 inches and the water surface elevations in both compartments noted. An observer continued to note the water surface elevation in the upstream compartment at predetermined time intervals. The permeability was calculated from the following equation:

$$K = \frac{LA_1}{A_m \alpha t} \ln \left(\frac{\alpha h_{1,0} - C_0}{\alpha h_1 - C_0} \right)$$

where L = length of media

$C_0 = h_{2,0} + \frac{A_1}{A_2} h_{1,0}$

A_1 = cross sectional area of the second compartment

A_2 = cross sectional area of the tidal compartment

h_1 = upstream head at any time, t

$h_{1,0}$ = upstream head initially

$h_{2,0}$ = downstream head initially

$\alpha = 1 + \frac{A_1}{A_2} = 2.0$

A_m = cross sectional area of media.

The results of several of these tests are presented in Figure B1-2

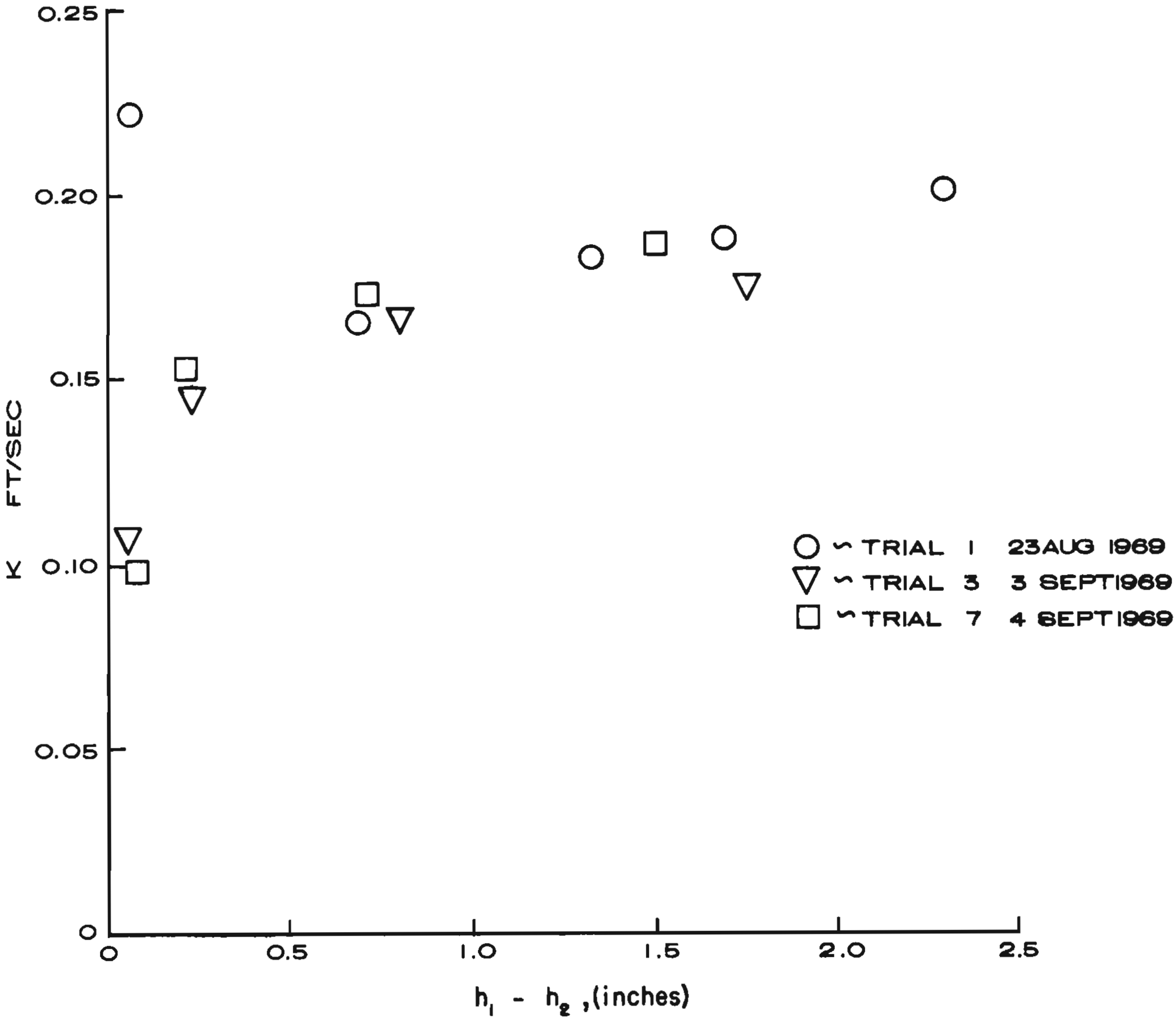

FIGURE B1-2. DARCY PERMEABILITY VS. HEAD DIFFERENCE FOR FALLING HEAD TESTS.

where K is plotted as a function of head difference (h_1 - h_2).

The results from all of the permeability tests are recorded in Table B1-1.

TABLE B1-1. SUMMARY OF RESULTS OF PERMEABILITY TESTS.

DATE	TEST CONDITIONS			FLOW DIRECTION	RANGE OF K FT./SEC.	AVERAGE K FT./SEC.
	APPARATUS	SAMPLE SIZE	TIME			
1 AUG. 69	PERMEAMETER TEST	2.875"D X 5.25"L	STEADY	Z	.099 - .158	.123
2 AUG. 69	"	" "	"	Z	.120 - .184	.145
5 AUG. 69	"	2.875"D X 6.25"L	"	Y	.145 - .151	.149
5 AUG. 69	"	2.875"D X 5.25"L	"	X	.129 - .167	.149
6 AUG. 69[1]	HYDRAULIC MODEL UNCONFINED	6"W X 12"H X 48"L	"	X	.255 - .262	.258
7 AUG. 69[1]	"	" "	"	X	.234 - .238	.237
14 AUG. 69[1]	"	" "	"	X	.169 - .193	.181
19 AUG. 69[2]	"	6"W X 6"H X 48"L	"	X	---	.291
20 AUG. 69[2]	HYDRAULIC MODEL CONFINED	2.875"W X 6"H X 50"L	"	X	---	.178
23 AUG. 69	"	" "	FALLING HEAD	X	.165 - .201	.170
3 SEPT. 69	"	5.875"W X 6"H X 50"L	"	X	.108 - .174	.170
3 SEPT. 69	"	" "	"	X	.071 - .205	.170
4 SEPT. 69[3]	"	" "	"	X	.097 - .187	.170

[1] HEAD MEASURED BY PRESSURE TRANSDUCER.
[2] HEAD MEASURED BY LEVEL AND POINT GAGE.
[3] SAME CONDITIONS AS TESTS ON 3 SEPT. EXCEPT SAMPLE HAD BEEN IN TANK FOR 24 HOURS PRIOR TO TEST.

SIZE AND ORIENTATION OF THE POLYURETHENE SHEET

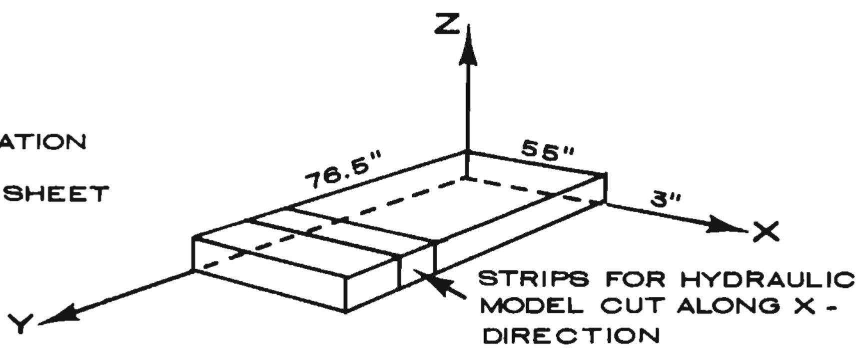

APPENDIX C

Calculation of the time-scale factor, K_4, for tests on KONA, 4 September 1969.

For KONA: $a = 2$ in , $S_s = 0.032$ ft $^{-1}$

For the tests on 4 September 1969: $b = 5.875$ in , $K = 0.21$ ft /sec for $T = 6$ sec

Thus, the storage and transmissibility become

$S = S_s b = 0.0155$, and

$T = Kb = 0.103$ ft /sec

Let $K_2 = 0.1$ ft /volt (this value was used in all electric analog model tests). Then from equation (15)

$K_3 = RTK_2 = 1.03 \times 10^{-2}$ R

A convenient value for R is 100 ohms, hence

$K_3 = 1.03$ ft^3 /amp-sec

From equation (16)

$$K_1 = \frac{a^2 S}{C} K_2 = 4.31 \times 10^{-4}\ C^{-1}.$$

A convenient value for C is 0.02×10^{-6} farads, hence

$K_1 = 2150$ ft^3 /coulomb

Thus, from equation (12) the time-scale factor is

$K_4 = K_1/K_3 = 2085$ hydraulic model seconds/electric analog seconds.

Specifically, a period of 6.0 seconds in the hydraulic model corresponds to 348 cps in the electric analog.

APPENDIX D

Computer programs and sample output for:

KONABAK	Data of 4 September 1969
KONA	Data of 4 September 1969
KOHA	Data of 3 September 1969
POCI	

KONABAK - 4 SEPTEMBER 1969

```
FORTRAN IV G LEVEL 1, MOD 4             MAIN              DATE = 70124          16/03/22

             C
             C
             C KONABAK  CALCULATES THE ARGUMENT, A, GIVEN RHO, AND X, BY USING THE
             C          NEWTON RAPHSON METHOD
             C
 0001            1 READ (5, 2) RHO, X
 0002            2 FORMAT (F6.3, F6.3)
             C TEST FOR SENTINEL CARD, RHO = 0.000
 0003              IF (RHO .EQ. 0.000) STOP
 0004              WRITE (6, 5) RHO, X
 0005            5 FORMAT (1HO, 6HAMP = , F6.3, 3X, 6HLOC = , F6.3/1HO, 5HALPHA)
 0006              A = 4.0
 0007              N = 1
 0008            3 COS2A = COS(A) ** 2
 0009              SINH2A = SINH(A) ** 2
 0010              COS2AX = COS(A * X) ** 2
 0011              SINH2X = SINH(A * X) ** 2
 0012              FX = (RHO ** 2) * (COS2A + SINH2A) - (COS2AX + SINH2X)
 0013              DFX = ((RHO ** 2) * (SINH(2 * A) - SIN(2 * A))) + (X * (SIN(2 * A
             C DFX = THE DERIVATIVE OF FX WITH RESPECT TO X
                  1* X) - SINH(2 * A * X)))
 0014              ANEW = A - (FX / DFX)
 0015              WRITE (6, 4) ANEW
 0016            4 FORMAT (1H , E13.6)
             C IF THE ABSOLUTE VALUE OF (A - ANEW) IS LESS THAN 1.0E-3 OR IF ANEW
             C HAS BEEN CALCULATED MORE THAN 50 TIMES, CALCULATE ANEW USING NEW
             C VALUES OF RHO AND X
             C
             C OTHERWISE, REPLACE A WITH ANEW AND CALCULATE ANEW AGAIN
 0017              IF (ABS(A - ANEW) .LT. 1.0E-3 .OR. N .GT. 90) GO TO 1
 0018              N = N + 1
 0019              A = ANEW
 0020              GO TO 3
 0021              END
```

AMP = 0.902 LOC = 0.760

ALPHA
0.352515E 01
0.305656E 01
0.259493E 01
0.214456E 01
0.172147E 01
0.135720E 01
0.108588E 01
0.928977E 00
0.877048E 00
0.871921E 00
0.871876E 00

AMP = 0.850 LOC = 0.520

ALPHA
0.350652E 01
0.301558E 01
0.252955E 01
0.205904E 01
0.163082E 01
0.128208E 01
0.104217E 01
0.922927E 00
0.894707E 00
0.893286E 00
0.893282E 00

AMP = 0.830 LOC = 0.280

ALPHA
0.350120E 01
0.300326E 01
0.250951E 01
0.203342E 01
0.160545E 01
0.126374E 01
0.103592E 01
0.930124E 00
0.908577E 00
0.907771E 00

AMP = 0.820 LOC = 0.040

ALPHA
0.350072E 01
0.300214E 01
0.250777E 01
0.203151E 01
0.160449E 01
0.126543E 01
0.104243E 01
0.942433E 00
0.923609E 00
0.923006E 00

AMP = 0.860 LOC = 0.760

ALPHA
0.352814E 01
0.306354E 01
0.260707E 01
0.216300E 01
0.174736E 01
0.139392E 01
0.114292E 01
0.101743E 01
0.988350E 00
0.986958E 00
0.986957E 00

AMP = 0.800 LOC = 0.520

ALPHA
0.350741E 01
0.301784E 01
0.253388E 01
0.206668E 01
0.164441E 01
0.130777E 01
0.109068E 01
0.100018E 01
0.985788E 00
0.985457E 00

AMP = 0.775 LOC = 0.280

ALPHA
0.350142E 01
0.300397E 01
0.251138E 01
0.203807E 01
0.161660E 01
0.128894E 01
0.108657E 01
0.100973E 01
0.999686E 00
0.999529E 00

AMP = 0.770 LOC = 0.040

ALPHA
0.350085E 01
0.300264E 01
0.250925E 01
0.203550E 01
0.161450E 01
0.128847E 01
0.108878E 01
0.101443E 01
0.100510E 01
0.100497E 01

AMP = 0.810 LOC = 0.760

ALPHA
0.353250E 01
0.307375E 01
0.262495E 01
0.219042E 01
0.178624E 01
0.144872E 01
0.122435E 01
0.113178E 01
0.111793E 01
0.111765E 01

AMP = 0.700 LOC = 0.520

ALPHA
0.350983E 01
0.302394E 01
0.254562E 01
0.208737E 01
0.168096E 01
0.137477E 01
0.120732E 01
0.116123E 01
0.115816E 01
0.115815E 01

AMP = 0.650 LOC = 0.280

ALPHA
0.350214E 01
0.300631E 01
0.251752E 01
0.205327E 01
0.165243E 01
0.136638E 01
0.122660E 01
0.119639E 01
0.119514E 01
0.119514E 01

AMP = 0.635 LOC = 0.040

ALPHA
0.350138E 01
0.300461E 01
0.251508E 01
0.205118E 01
0.165320E 01
0.137344E 01
0.124161E 01
0.121532E 01
0.121439E 01

AMP = 0.700 LOC = 0.760

ALPHA
0.354689E 01
0.310783E 01
0.268566E 01
0.228594E 01
0.192542E 01
0.164387E 01
0.149069E 01
0.145310E 01
0.145120E 01
0.145119E 01

AMP = 0.520 LOC = 0.520

ALPHA
0.351840E 01
0.304572E 01
0.258770E 01
0.216155E 01
0.180892E 01
0.158956E 01
0.151677E 01
0.151006E 01
0.151001E 01

AMP = 0.470 LOC = 0.280

ALPHA
0.350436E 01
0.301350E 01
0.253629E 01
0.209888E 01
0.175488E 01
0.156296E 01
0.151160E 01
0.150845E 01
0.150844E 01

AMP = 0.460 LOC = 0.040

ALPHA
0.350289E 01
0.301019E 01
0.253140E 01
0.209420E 01
0.175392E 01
0.156845E 01
0.152119E 01
0.151856E 01
0.151855E 01

```
AMP =  0.560   LOC =  0.760

ALPHA
 0.358809E 01
 0.320809E 01
 0.287155E 01
 0.259544E 01
 0.240455E 01
 0.231702E 01
 0.230101E 01
 0.230054E 01

AMP =  0.350   LOC =  0.520

ALPHA
 0.354329E 01
 0.310953E 01
 0.271235E 01
 0.238071E 01
 0.216395E 01
 0.208554E 01
 0.207727E 01
 0.207719E 01

AMP =  0.250   LOC =  0.280

ALPHA
 0.351628E 01
 0.305165E 01
 0.263277E 01
 0.231500E 01
 0.215773E 01
 0.212694E 01
 0.212595E 01

AMP =  0.230   LOC =  0.040

ALPHA
 0.351241E 01
 0.304483E 01
 0.262864E 01
 0.232558E 01
 0.218979E 01
 0.216808E 01
 0.216760E 01
```

KONA - 4 SEPTEMBER 1969

```
FORTRAN IV G LEVEL 1, MOD 4            MAIN              DATE = 70124          14/44/21

              C
              C
              C KONA      CALCULATES THE AMPLITUDES AND PHASE ANGLES FOR A ONE
              C           DIMENSIONAL CONFINED AQUIFER WITH NO FLOW BOUNDARY CONDITIONS
              C
 0001            10 READ (5, 1) PERIOD, T
              C T = TRANSMISSIBILITY
 0002             1 FORMAT (F5.0, F7.4)
              C TEST FOR SENTINEL CARD,  PERIOD = 18.0
 0003               IF (PERIOD .EQ. 18.0) STOP
              C ALPHA = (SQRT((S*SIGMA)/(T*2.0)))*L
              C S = STORAGE COEFFICIENT = 0.0155
              C SIGMA = FREQUENCY = (2*PI)/PERIOD RAD/SEC
              C L = LENGTH = 4.167 FT
 0004               SIGMA = 6.2831583 / PERIOD
 0005               ALPHA = (SQRT((0.0155 * SIGMA) / (T * 2.0))) * 4.167
 0006               WRITE (6, 2) ALPHA
              C FORMAT PRINTS HEADINGS,  LOC  AMP  PHASE
 0007             2 FORMAT (1H1, 6HARG = , F6.3/4H0LOC, 5X, 3HAMP, 7X, 5HPHASE)
              C CALCULATE AND PRINT THE AMPLITUDES AND PHASE ANGLES FOR VALUES OF X
              C BETWEEN 0.0 AND 1.0 INCLUSIVELY, INCREMENTING X BY 0.1
              C RHO = AMPLITUDE
              C DEGREE = PHASE ANGLE
              C X = LOCATION
 0008               TENX = 0.0
 0009            20 X = TENX / 10.0
 0010               RHO = SQRT(((COS(ALPHA * X) ** 2) + (SINH(ALPHA * X) ** 2)) /
                   1((COS(ALPHA) ** 2) + (SINH(ALPHA) ** 2)))
 0011               TAM = ((TANH(ALPHA * X) * TAN(ALPHA * X)) - (TANH(ALPHA) *
                   2TAN(ALPHA))) / (1 + (TANH(ALPHA * X) * TAN(ALPHA * X) *
                   3TANH(ALPHA) * TAN(ALPHA)))
 0012               THETA = ATAN(TAM)
 0013               DEGREE = THETA * (360 / 6.2831853)
 0014               WRITE (6, 3) X, RHO, DEGREE
 0015             3 FORMAT (1H0, F3.1, F10.3, F12.3)
              C X IS PRINTED UNDER LOC HEADING
              C RHO IS PRINTED UNDER AMP HEADING
              C DEGREE IS PRINTED UNDER PHASE HEADING
 0016               IF (X .GE. 1.0) GO TO 10
              C IF X = 1.0 START LOOP AGAIN WITH NEW ALPHA
 0017               TENX = TENX + 1.0
 0018               GO TO 20
 0019               END
```

ARG = 0.893

LOC	AMP	PHASE
0.0	0.837	-41.548
0.1	0.837	-41.091
0.2	0.837	-39.720
0.3	0.839	-37.437
0.4	0.842	-34.254
0.5	0.848	-30.198
0.6	0.860	-25.323
0.7	0.879	-19.720
0.8	0.907	-13.520
0.9	0.947	-6.886
1.0	1.000	0.0

ARG = 0.979

LOC	AMP	PHASE
0.0	0.786	-48.241
0.1	0.786	-47.691
0.2	0.787	-46.044
0.3	0.788	-43.304
0.4	0.792	-39.489
0.5	0.801	-34.646
0.6	0.817	-28.867
0.7	0.842	-22.299
0.8	0.880	-15.143
0.9	0.932	-7.633
1.0	1.000	0.0

ARG = 1.170

LOC	AMP	PHASE
0.0	0.664	-62.770
0.1	0.664	-61.986
0.2	0.664	-59.636
0.3	0.667	-55.734
0.4	0.674	-50.333
0.5	0.689	-43.563
0.6	0.715	-35.663
0.7	0.757	-26.979
0.8	0.817	-17.911
0.9	0.897	-8.830
1.0	1.000	0.0

ARG = 1.516

LOC	AMP	PHASE
0.0	0.461	-86.556
0.1	0.461	-85.239
0.2	0.462	-81.295
0.3	0.468	-74.790
0.4	0.482	-65.963
0.5	0.510	-55.343
0.6	0.557	-43.727
0.7	0.628	-31.953
0.8	0.725	-20.614
0.9	0.849	-9.965
1.0	1.000	0.0

ARG = 2.144

LOC	AMP	PHASE
0.0	0.236	56.424
0.1	0.236	59.057
0.2	0.238	66.898
0.3	0.249	79.456
0.4	0.275	-84.791
0.5	0.324	-68.148
0.6	0.399	-52.377
0.7	0.503	-37.994
0.8	0.635	-24.746
0.9	0.799	-12.199
1.0	1.000	0.0

KONA, 3 SEPTEMBER 1969

```
FORTRAN IV G LEVEL 1, MOD 4             MAIN              DATE = 70124          15/00/47

                C
                C
                C KOHA      CALCULATES THE AMPLITUDES AND PHASE ANGLES FOR A ONE
                C           DIMENSIONAL CONFINED AQUIFER WITH CONSTANT HEAD BOUNDARY
                C           CONDITIONS
                C
 0001              10 READ (5, 1) PERIOD, T
                C T = TRANSMISSIBILITY
 0002               1 FORMAT (F5.0, F7.4)
                C TEST FOR SENTINEL CARD,  PERIOD = 18.0
 0003                 IF (PERIOD .EQ. 18.0) STOP
                C ALPHA = (SQRT((S*SIGMA)/(T*2.0)))*L
                C S = STORAGE COEFFICIENT = 0.0155
                C SIGMA = FREQUENCY = (2*PI)/PERIOD RAD/SEC
                C L = LENGTH = 4.167 FT
 0004                 SIGMA = 6.2831583 / PERIOD
 0005                 ALPHA = (SQRT((0.0155 * SIGMA) / (T * 2.0))) * 4.167
 0006                 WRITE (6, 2) ALPHA
                C FORMAT PRINTS HEADINGS,  LOC  AMP  PHASE
 0007               2 FORMAT (1H1, 6HARG = , F6.3/4H0LOC, 5X, 3HAMP, 7X, 5HPHASE)
                C CALCULATE AND PRINT THE AMPLITUDES AND PHASE ANGLES FOR VALUES OF X
                C BETWEEN 0.0+ AND 1.0+ INCLUSIVELY, INCREMENTING X BY APPROXIMATELY
                C 0.1
                C RHO = AMPLITUDE
                C DEGREE = PHASE ANGLE
 0008                 TENX = 1.0E-10
 0009              20 X = TENX / 10.0
 0010                 RHO = SQRT(((SIN(ALPHA * X) ** 2) + (SINH(ALPHA * X) ** 2)) /
                     1((SIN(ALPHA) ** 2) + (SINH(ALPHA) ** 2)))
 0011                 COTHA = 1.0 / TANH(ALPHA)
 0012                 COTHAX = 1.0 / TANH(ALPHA * X)
 0013                 TAM = ((COTHAX * TAN(ALPHA * X)) - (COTHA * TAN(ALPHA))) /
                     1(1 + (COTHAX * TAN(ALPHA * X) * COTHA * TAN(ALPHA)))
 0014                 THETA = ATAN(TAM)
 0015                 DEGREE = THETA * (360 / 6.2831853)
 0016                 WRITE (6, 3) X, RHO, DEGREE
 0017               3 FORMAT (1H0, F3.1, F10.3, F12.3)
                C X IS PRINTED UNDER LOC HEADING
                C RHO IS PRINTED UNDER AMP HEADING
                C DEGREE IS PRINTED UNDER PHASE HEADING
 0018                 IF (X .GE. 1.0) GO TO 10
                C IF X IS GREATER THAN OR EQUAL TO 1.0 START LOOP AGAIN WITH NEW ALPHA
 0019                 TENX = TENX + 1.0
 0020                 GO TO 20
 0021                 END
```

ARG = 0.979

LOC	AMP	PHASE
0.0	0.000	-18.169
0.1	0.098	-17.986
0.2	0.196	-17.437
0.3	0.294	-16.522
0.4	0.392	-15.241
0.5	0.491	-13.594
0.6	0.590	-11.585
0.7	0.689	-9.215
0.8	0.791	-6.489
0.9	0.894	-3.414
1.0	1.000	0.0

ARG = 1.896

LOC	AMP	PHASE
0.0	0.000	-62.866
0.1	0.079	-62.179
0.2	0.158	-60.120
0.3	0.238	-56.692
0.4	0.319	-51.911
0.5	0.403	-45.816
0.6	0.492	-38.486
0.7	0.591	-30.046
0.8	0.704	-20.675
0.9	0.838	-10.585
1.0	1.000	0.0

ARG = 1.341

LOC	AMP	PHASE
0.0	0.000	-33.457
0.1	0.093	-33.114
0.2	0.187	-32.084
0.3	0.281	-30.368
0.4	0.374	-27.968
0.5	0.469	-24.890
0.6	0.566	-21.142
0.7	0.665	-16.744
0.8	0.769	-11.725
0.9	0.880	-6.126
1.0	1.000	0.0

ARG = 2.527

LOC	AMP	PHASE
0.0	0.000	80.582
0.1	0.057	81.801
0.2	0.115	85.456
0.3	0.173	-88.476
0.4	0.234	-80.079
0.5	0.302	-69.557
0.6	0.382	-57.271
0.7	0.482	-43.709
0.8	0.611	-29.387
0.9	0.780	-14.728
1.0	1.000	0.0

POCI

```
FORTRAN IV G LEVEL 1, MOD 4            MAIN               DATE = 70124          14/59/44

              C
              C
              C POCI     CALCULATES THE AMPLITUDES AND PHASE ANGLES FOR AN UNCONFINED
              C            CYLINDRICAL ISLAND AQUIFER
              C
              C      SAR = SQRT((EPSI*SIGMA*(RB**2))/(K*Z))
              C EPSI = POROSITY
              C SIGMA = FREQUENCY
              C RB = RADIUS OF THE ISLAND
              C K = PERMEABILITY
              C Z = EQUILIBRIUM POSITION
 0001            10 READ (5, 1) SAR
 0002             1 FORMAT (F6.3)
              C TEST FOR SENTINEL CARD, SAR = 0.000
 0003               IF (SAR .EQ. 0.000) STOP
 0004               WRITE (6, 2) SAR
              C FORMAT PRINTS HEADINGS,  LOC  AMP  PHASE
 0005             2 FORMAT (1H1, 6HARG = , F6.3/4H0LOC, 5X, 3HAMP, 7X, 5HPHASE)
              C CALCULATE AND PRINT THE AMPLITUDES AND PHASE ANGLES FOR VALUES OF X
              C BETWEEN 0.0 AND 0.9 INCLUSIVELY, INCREMENTING X BY 0.1
              C X = LOCATION
              C RHO = AMPLITUDE
              C DEGREE = PHASE ANGLE
 0006               TENR = 0.0
 0007            20 R = TENR / 10.0
 0008               A = SAR
 0009               AX = SAR * R
 0010               CALL CALBER (BER1, AX)
 0011               CALL CALBER (BER2, A)
 0012               CALL CALBEI (BEI1, AX)
 0013               CALL CALBEI (BEI2, A)
 0014               BER12 = BER1 ** 2
 0015               BER22 = BER2 ** 2
 0016               BEI12 = BEI1 ** 2
 0017               BEI22 = BEI2 ** 2
 0018               RHO = SQRT((BER12 + BEI12) / (BER22 + BEI22))
 0019               THETA = ATAN(((BER2 * BEI1) - (BEI2 * BER1)) / ((BER1 * BER2) +
                   1(BEI1 * BEI2)))
 0020               DEGREE = THETA * (360 / 6.2831853)
 0021               WRITE (6, 3) R, RHO, DEGREE
 0022             3 FORMAT (1H0, F3.1, F10.3, F12.3)
              C X IS PRINTED UNDER LOC HEADING
              C RHO IS PRINTED UNDER AMP HEADING
              C DEGREE IS PRINTED UNDER PHASE HEADING
 0023               IF (R .GE. 0.9) GO TO 10
              C IF X = 0.9 START LOOP AGAIN WITH NEW ALPHA
 0024               TENR = TENR + 1.0
 0025               GO TO 20
```

```
FORTRAN IV G LEVEL 1, MOD 4            CALBER             DATE = 70124          14/59/44

 0001               SUBROUTINE CALBER (BER, X)
              C SUBROUTINE CALBER CALCULATES THE BER FUNCTION WITH ARGUMENT X, USING
              C THE SERIES REPRESENTATION OF BER.
 0002               BER = 1.0
 0003               TERM = 1.0
 0004               DO 3 I = 1, 100
 0005               TI2 = (2 * I) ** 2
 0006               TIP12 = ((2 * I) - 1) ** 2
 0007               XX = ((0.25) * (X ** 2)) ** 2
 0008               Y = ((-1) * XX) / (TI2 * TIP12)
 0009               TERM = TERM * Y
 0010               BER = BER + TERM
 0011               IF (ABS(TERM) .LE. 1.0E-5) GO TO 4
 0012             3 CONTINUE
 0013             4 RETURN
 0014               END
```

```
FORTRAN IV G LEVEL 1, MOD 4            CALBEI            DATE = 70124

 0001                 SUBROUTINE CALBEI (BEI, X)
             C SUBROUTINE CALBEI CALCULATES THE BEI FUNCTION WITH ARGUMENT X, USING
             C THE SERIES REPRESENTATION OF BEI.
 0002                 TERM = 0.25 * (X ** 2)
 0003                 BEI = 0.25 * (X ** 2)
 0004                 DO 3 I = 1, 100
 0005                 TI2 = (2 * I) ** 2
 0006                 TIM12 = ((2 * I) + 1) ** 2
 0007                 XX = ((0.25) * (X ** 2)) ** 2
 0008                 Y = ((-1) * XX) / (TI2 * TIM12)
 0009                 TERM = TERM * Y
 0010                 BEI = BEI + TERM
 0011                 IF (ABS(TERM) .LE. 1.0E-5) GO TO 4
 0012               3 CONTINUE
 0013               4 RETURN
 0014                 END
```

ARG = 1.158

LOC	AMP	PHASE
0.0	0.973	-18.975
0.1	0.973	-18.783
0.2	0.973	-18.207
0.3	0.973	-17.247
0.4	0.974	-15.903
0.5	0.975	-14.177
0.6	0.977	-12.072
0.7	0.980	-9.592
0.8	0.984	-6.744
0.9	0.991	-3.542

ARG = 1.637

LOC	AMP	PHASE
0.0	0.903	-36.683
0.1	0.903	-36.299
0.2	0.903	-35.148
0.3	0.904	-33.230
0.4	0.906	-30.549
0.5	0.909	-27.117
0.6	0.916	-22.953
0.7	0.927	-18.093
0.8	0.944	-12.594
0.9	0.968	-6.531

ARG = 1.337

LOC	AMP	PHASE
0.0	0.953	-25.067
0.1	0.953	-24.811
0.2	0.953	-24.043
0.3	0.954	-22.763
0.4	0.955	-20.973
0.5	0.956	-18.675
0.6	0.959	-15.876
0.7	0.965	-12.587
0.8	0.973	-8.826
0.9	0.984	-4.618

ARG = 2.316

LOC	AMP	PHASE
0.0	0.719	-66.425
0.1	0.719	-65.657
0.2	0.720	-63.353
0.3	0.722	-59.521
0.4	0.727	-54.194
0.5	0.739	-47.450
0.6	0.760	-39.438
0.7	0.794	-30.390
0.8	0.843	-20.600
0.9	0.911	-10.379